AN ABSTRACT OF THE THESIS OF

M. Pilar Cornejo-Rodriguez for the degree of Master of Science in Oceanography presented on March 4, 1987.

Title: Propagation and Forcing of High Frequency Sea Level Variability in the Eastern Equatorial Pacific.

Abstract approved: David B. Enfield

Sea level and wind data from coastal and island stations from Buenaventura, Colombia (4°N) to Callao, Peru (12°S) have been analyzed for the 1979-1984 time period, to describe the seasonal and interannual variations in the characteristics of short time scale variability (1-2 weeks). Auto- and cross spectral analyses are used to make comparisons between Austral summers and winters as well as interannual comparisons between the 1982-1983 El Niño/Southern Oscillation (ENSO) period and non-ENSO years. The principal results show weak evidence of local forcing of the sea level by the alongshore wind during the whole year without significant differences between summer and winter seasons. The alongshore coherence and phase spectra between the sea level series show evidence of poleward propagating fluctuations at speeds of 2.6-3.0 ms^{-1} during winter, but no propagation is evident during summer. There is also a large energy increase in coastal sea level, especially in the 8-11 day band, during the 1982-1983 ENSO episode.

This increase is associated with a non-dispersive, poleward propagation of events at speeds of 3.4-3.6 ms^{-1}. The propagating fluctuations are superimposed on a weak, locally forced variability. The only plausible source for the observed coastal fluctuations appears to be trapped waves in the equatorial waveguide. Additional equatorial data from subsurface pressure gauges in the Galapagos Islands and inverted echo sounders at 3°N,95°W, 3°N,85°W and 2°S,85°W are used to explore the possibility that the coastal signal during the 1982-1983 ENSO episode is connected to the arrival of energy in the form of equatorially trapped Rossby-gravity (Yanai) and Kelvin waves, and to determine the respective contributions of the two wave types. Cross spectral analyses, frequency domain EOF analysis and the characteristics of equatorial waves demonstrate that equatorially trapped Yanai waves are the principal source of the propagating signals in the coastal sea levels during the 1982-1983 ENSO. During the 1982-1983 ENSO, between 64% and 91% of the coastal SLH variability in the 8-11 day period band is associated with antisymmetric variability across the equator. Phase in this band is zonally invariant along the equator but is poleward propagating along the coast, consistent with the conversion of stationary, equatorial Yanai waves into coastal trapped waves.

Propagation and Forcing of High Frequency Sea Level Variability in the Eastern Equatorial Pacific

by

M. Pilar Cornejo-Rodriguez

A THESIS

submitted to

Oregon State University

in partial fulfillment of
the requirements for the
degree of

Master of Science

Completed March 4, 1987

Commencement June 1987

APPROVED: Redacted for privacy

Professor of Oceanography in charge of major

Redacted for privacy

Dean of the College of Oceanography

Redacted for privacy

Dean of Graduate School

Date thesis is presented March 4, 1987

Type by researcher for M. Pilar Cornejo-Rodriguez

ACKNOWLEDGEMENTS

I want to thank my thesis advisor, Dr. D.B. Enfield, for his considerable help and assistance. We also want to acknowledge the helpful discussions of this research provided by R.L. Smith, A. Huyer, P.M. Newberger and T. Paluszkiewicz. We thank H. Pittock for his assistance in processing the data. We also express our gratitude to the organizations in North and South America, cited in Table II.1 and Table III.1, that provided the coastal and equatorial data for this research. This research was performed with the support of the National Science Foundation Grant OCE-8317390 and National Oceanic and Atmospheric Administration Grant No. NA85AA--CA024.

TABLE OF CONTENTS

LIST OF FIGURES

LIST OF TABLES

Propagation and Forcing of High Frequency Sea Level Variability in the Eastern Equatorial Pacific

CHAPTER I

INTRODUCTION

There now exists a large body of theoretical and observational evidence to support the existence of long wave propagation along the eastern Pacific boundary at both high and low frequencies. Some of the coastal variability at high frequencies (days to weeks) is locally forced, while at certain times and places it appears to be remotely forced at more equatorward coastal locations, (e.g., Wang and Mooers, 1973; Enfield and Allen, 1983; Halliwell and Allen, 1984). At low frequencies the equatorial zone is the primary source of the remotely forced variability found along the coastal boundary. This has been demonstrated, for example, for the interannual El Niño disturbances (Enfield and Allen ,1980; Chelton and Davis, 1982) and was more recently shown to be true at intraseasonal periods (40-60 days) as well (Enfield, 1987).

At high frequencies, in the days-weeks period range, a number of researchers have identified and described poleward propagating fluctuations that traveled along the Peru coast at 2-3 m s^{-1} during the moderate 1976-1977 El Niño/Southern Oscillation (ENSO) event (e.g, Smith, 1978; Brink, 1982; Romea and Smith, 1983). The coastal fluctuations have the characteristics of low-latitude, baroclinic coastal trapped waves. These studies find that the fluctuations are

predominantly unforced by the local alongshore wind between 5°S and 15°S; however, they lacked wind data closer to the equator with which to test for a more northern coastal forcing . Because all of the studies of the Peru variability are based on data taken during a moderate ENSO event (1976-1977), the question of the existence of similar propagating variability or of coastal forcing during non-ENSO periods is still unanswered, as are questions of seasonal variability.

No convincing source, equatorial or coastal, has been demonstrated for these propagating fluctuations. Romea and Smith (1983) tried to establish a link between the coastal fluctuations in the days-weeks band and equatorial variability by comparing one tide station in the Galapagos Islands (Baltra Island, 27 nautical miles south of the equator) with the stations along the Peru coast. They found only tenuous evidence to support equatorially trapped Kelvin waves as the source for the coastal propagating signals.

Several studies in the equatorial region surrounding the Galapagos Islands (e.g., Ripa and Hayes, 1981; Chiswell et al, 1987) suggest that equatorial variability in the days-weeks period band consists of energy in the form of equatorially trapped Rossby-gravity (Yanai) waves, as well as Kelvin waves. Yanai waves, unlike Kelvin waves, have an antisymmetric surface displacement structure about the equator; therefore, if they are an important source of variability, off-equatorial oceanic data is required to detect them. This would explain why Romea and Smith (1983), who

lacked off-equatorial oceanic data, failed to demonstrate a clear equatorial connection to the coastal variability. Ripa and Hayes (1981) apply a time domain EOF analysis to sea level height series from subsurface pressure gauges located in the Galapagos Islands. They find that the first (second) mode was in agreement with the symmetric (antisymmetric) structure of Kelvin (Yanai) waves, with the Kelvin (Yanai) waves dominating at the lower (higher) frequencies. Chiswell et al (1987) analyze the dynamic height series from inverted echo sounders at off-equatorial stations surrounding the Galapagos and find evidence of both Kelvin and Yanai waves during the 1982-1983 ENSO event, with the latter being especially strong in the 6-10 day period range.

Our main interest is to describe the seasonal and interannual variations in the characteristics of short time scale variability (1-2 weeks) of sea level in the 1979-1984 period and to document the nature of local wind forcing along the coast, especially in the near-equatorial zone not addressed by previous studies. We also explore the possibility that the coastal variability is connected to the arrival of energy in the form of equatorially trapped Rossby-gravity (Yanai) as well as Kelvin waves; we now have sufficient data from equatorial and coastal stations to establish such a connection, as well as the relative contributions of the two wave types.

In Chapter II we use estimates of sea surface height from coastal tide gauges and coastal winds from synoptic weather stations

in Colombia, Ecuador, Peru and the Galapagos for the 1979-1984 period to determine the propagation and forcing of high frequency (days to weeks) sea level variability along the west coast of South America. Auto- and cross spectral analyses are used to make comparisons between austral summers and winters for non-ENSO periods. We also make interannual comparisons between ENSO and non-ENSO periods, and design our studies to bracket the 1982-1983 ENSO event. We find that the energy, alongshore coherence and phase propagation (3-4 m s^{-1}) in the coastal sea level are stronger in the 8-11 day period band during the 1982-1983 ENSO than either before or after the event. The cross spectra between wind and sea level indicate that some local forcing probably occurs but the principal source for the energetic propagating signal in coastal sea level appears to be in the equatorial waveguide.

In Chapter III we have used additional equatorial data from subsurface pressure gauges in the Galapagos (Ripa and Hayes, 1981) and inverted echo sounders at 3°N,95°W, 3°N,85°W and 2°S,85°W (Chiswell et al, 1987) for the 1982-1983 period. Cross spectral analyses, frequency domain EOF analysis and the characteristics of equatorial waves are used to determine the existence and nature of the dynamical connection between the observed coastal variability and incident equatorial disturbances for periods between several days and two weeks. Our analyses demonstrate that equatorially trapped Yanai waves are the principal source of the propagating signals in the coastal sea level during the 1982-1983 ENSO.

CHAPTER II

PROPAGATION AND FORCING OF HIGH FREQUENCY SEA LEVEL VARIABILITY ALONG THE WEST COAST OF SOUTH AMERICA

ABSTRACT

Tide and wind data from coastal and island stations from Buenaventura, Colombia (4°N) to Callao, Peru (12°S) have been analyzed for the 1979-1984 time period to determine the propagation and forcing characteristics of coastal trapped waves at periods of days to weeks, as well as how they vary either with season or between the 1982-1983 El Niño/Southern Oscillation (ENSO) period and non-ENSO years. During four non-ENSO years, the ensemble averaged cross spectra between coastal sea level height (SLH) and local winds show weak evidence of local forcing during the whole year without significant differences between Austral summer and winter seasons. Cross spectra between SLH series from neighboring stations show some evidence of poleward propagating fluctuations during winter seasons at speeds of 2.6-3.0 m s^{-1} but no propagation is found during summer. During the 1982-1983 ENSO there is a large increase in energy at most frequencies, but especially in the 8-11 day band at all coastal stations, where energies are enhanced by as much as an order of magnitude above non-ENSO levels. The cross

spectra between adjacent SLH stations indicate a non-dispersive poleward propagation of events during the 1982-1983 ENSO with phase speeds of 3.4-3.6 ms^{-1}. As with the SLH energy, the coherence and phase propagation are much stronger in 1982-1983 than during non-ENSO periods, especially in the 8-11 day band. The 60% increase in phase speed during ENSO over the non-ENSO speed is consistent with the anomalous depression of the density structure that occurred during the EL Niño. Comparisons between coastal SLH and the local alongshore wind suggest that locally forced SLH variability was weak during the 1982-1983 ENSO and that energetic, propagating fluctuations were probably remotely forced in the equatorial waveguide.

II.1 INTRODUCTION

Theoretical results indicate that when low frequency equatorially trapped waves impinge on the eastern boundary they may be partially transmitted poleward along the coast in the form of coastally trapped waves (Moore, 1968), and partially reflected westward into the low-latitude ocean interior as Rossby waves. For typical equatorial stratification, however, the Rossby reflections are only possible at periods of 25-30 days and longer. This provides us with a working definition of "low-frequency". At shorter periods of a week or less, equatorial inertia-gravity waves (Wunsch and Gill, 1976; Luther 1980) are capable of reflecting energy westward. For periods of 5-7 days to 3-4 weeks, however, only eastward propagating energy is possible along the equator. This takes the form of Kelvin waves or mixed Rossby-gravity (Yanai) waves. When these waves arrive at the eastern boundary, all their energy is channeled poleward as coastal trapped waves (Clarke, 1983). It is this intermediate period range that has been frequently studied for the Peru coast and is the main subject of this paper.

Smith (1978), Brink et al (1978), Brink (1982) and Romea and Smith (1983) have analyzed fluctuations in the sea level and currents along the Peru coast during the 1976-1977 ENSO event. They find that fluctuations in the days-weeks band propagate poleward at

speeds of 2-3 m s^{-1}. These results are consistent with first baroclinic mode coastal trapped waves, which at low latitudes look much like coastal Kelvin waves (Allen and Romea, 1980, Brink 1982). Romea and Smith (1983) applied a frequency domain EOF analysis to horizontal and vertical current meter arrays in an alongshore coherent band of 0.1-0.2 cycles per day (cpd). Their analysis reveals the presence of modes with poleward phase propagation (2.5-2.7 m s^{-1}) that explain more than 70% of the variance in this band. They also find that there was little or no coherence between these fluctuations in either the alongshore currents or sea level and the local winds from 5°S to 15°S along the Peruvian coast, suggesting a remote source. They lacked the data to determine whether the local forcing varies seasonally or interannually, and could not check on the possibility of coastal forcing north of 5°S. None of the previous studies of the Peru coast have covered non-ENSO periods, hence do not show whether strong propagating variability is a permanent feature of the Peru coastal system.

In this study we use auto- and cross spectral analyses of six years of sea level and wind data to determine the forcing and propagation of synoptic time scale variability along the west coast of South America from Colombia to Peru (Figure II.1). We want to establish, if possible, the differences between Austral summers and winters for non-ENSO periods and to compare the variability between ENSO and non-ENSO periods. We have therefore designed our study to bracket the 1982-1983 ENSO, as well as the normal periods before and

after the event.

The most important results are that the energy, alongshore coherence and phase propagation in the coastal sea levels were more strongly developed during the 1982-1983 ENSO event over a wide range of frequencies, especially in the 8-11 day band, and significantly less so before and after the event. In addition, the coherence and phase spectra between sea level and local winds at the coastal stations show weak evidence of local forcing that is obscured by the more energetic, remotely forced variability, especially during the ENSO period. The only plausible source of the propagating fluctuations appears to be trapped waves in the equatorial waveguide whose energy impinges on the eastern boundary.

II.2 DATA SETS

The data sets consist of time series of up to six years of coastal wind and sea level height (SLH) that have been obtained from three synoptic weather stations and five tide gauges along the west coast of South America and in the Galapagos Islands (Figure II.1, Table II.1).

To remove the diurnal signal and tides from the data, the time series were smoothed with a Cosine-Lanczos filter (low-low pass = LLP) having half-amplitude near 40 hours and then decimated to 12 hourly intervals. To represent the forcing we rotate the wind in

accordance with the local coastline orientation and use the alongshore component. The SLH and wind LLP series are shown in Figure II.2 with the means removed. For the wind series the means are northward at all stations: 1.9 ms^{-1}, 6.4 ms^{-1} and 2.7 ms^{-1} at La Libertad, Talara and Callao, respectively. Surface atmospheric pressure from nearby meteorological stations was added to the SLH series to produce "adjusted" sea level at all stations except Santa Cruz (which is not used in our statistical analyses). The barometrically adjusted sea level is an approximation to the subsurface water pressure, which is the most dynamically relevant form of sea level. To remove low frequency variability from the LLP time series we applied a very low pass (VLP) filter with a half-amplitude near 30 days and subtracted to form the band-passed (LLP-VLP) series shown in Figure II.3.

The 1982-1984 data from a tide gauge installed under the National Oceanic and Atmospheric Administration's Equatorial Pacific Ocean Climate Studies (EPOCS) program at Paita (5°S) was spliced by regression to the 1979-1981 data from Talara, (less than 50 km to the north), which subsequently deteriorated badly in quality and continuity. For the 1982-1984 period, 25 months of data are from Paita and 11 months from Talara. We refer to the combined series as Talara-Paita. Two short gaps (December 1980, 15 days; and March 1984, 9 days) in the winds at Talara were filled with an autoregressive prediction filter that introduces fictitious values having statistical characteristics similar to the data on either

side of the gap. There were two one-month gaps in the Talara-Paita sea level series. The first gap (February 1979) does not interfere with our analyses, hence, it has not been filled. The second gap (March 1980) was filled by regression on the La Libertad SLH series. The various data fills were necessary in order to perform the spectral calculations but constitute less than 8% of the shortest series lengths analyzed. We have tested the effects of filling similar (artificially introduced) gaps in complete time series and find no significant differences from the analysis of unaltered data.

For the analysis of the seasonal differences we define the Austral winter (summer) as extending from mid-May to mid-November (mid-November to mid-May), which is the approximate period of strong (weak) southeast trade winds. For differences between years, we center the analyses on the 1982-1983 ENSO event and define three 13-month periods: Pre-ENSO (June 1981 through June 1982); ENSO (September 1982 through September 1983); and Post-ENSO (December 1983 through December 1984). The temporal distributions of these seasonal and interannual periods are shown in Figure II.2.

II.3 DESCRIPTION OF THE TIME SERIES

Comparing the SLH series (Figure II.2, bottom), we notice that an annual cycle is present at Buenaventura but totally absent on or south of the equator. There is also a clear interannual variation

in SLH at all stations. During the 1982-1983 ENSO event there is a period of increased SLH in the time series, which appears as two separated peaks in all cases.

The annual cycle is evident in the wind series (Figure II.2, top), with a stronger signal at Talara than at Salinas or Lima. The annual cycles at Talara and Salinas are in phase with each other and out of phase with Lima winds. This agrees with the analysis of 22-30 years of coastal winds by Enfield (1981a), who found that some of the coastal stations are in phase with the southeast trades, e.g., Talara (minimum during the Austral summer, maximum during the winter), and others out of phase, e.g, Lima (maximum during the Austral summer, minimum during the winter). Enfield and Newberger (1984) have shown that there was little indication of anomalous activity in the winds during the last quarter of 1982, even though El Niño conditions had already begun in the eastern Pacific. Anomalous conditions developed during 1983 (Figure II.2) indicated by a weakening in the monthly means at Talara and Salinas, and an increase in the winds at Lima. This, too, is consistent with the analysis of many years of data (Enfield 1981a,b).

Because of our interest in the shorter period variability, we wish to inquire as to whether the statistics of the residual (VLP-LLP) sea level series change from season to season or from year to year, or even independent of the low frequency variations noted above. During the 1982-1983 ENSO event there is an increase in the amplitudes of the residual SLH series (Figure II.3) evident at the

coastal stations but not at Santa Cruz. Comparisons between the ENSO period and the pre- and post-ENSO ones show that the rms amplitudes of the residual series are 2-4 times larger during the ENSO episode than those corresponding to periods before and after the event at all coastal stations south of the equator (Table II.2). During 1979-1981 and 1984 (not shown in Figure II.3 for added clarity) the amplitudes are similar to the first nine months of 1982 and there are no detectable seasonal or interannual modulations of the fluctuation amplitudes, i.e., the data appear to be stationary. Hence, the visual impression gained from the data is one of seasonal stationarity at the higher frequencies and strong non-stationarity between ENSO and non-ENSO years.

II.4 FORCING AND PROPAGATION: COMPARISONS BETWEEN SEASONS

II.4.1 Autospectra

To quantitatively compare the characteristics of the fluctuations for eacseone separately computed the autospectra in the LLP wind and SLH series for non-ENSO summers and winters (Figure II.2). We ensemble-averaged the four sets oa spectral estimates for each season, yielding eight degrees of freedom (df) at each frequency. To smooth the composite spectra we then applied a four

point running band average on two neighboring frequencies with one overlapping frequency, obtaining 16 df per band and a bandwidth of 0.011 day^{-1} (cpd). As an example, we show the autospectra for the Talara-Paita wind and SLH series in Figure II.4. For clarity, the autospectra for summers have been offset by two decaea 1 with respect to the winter spectra. As a reference level we have drawn a line with a slope of -5/3 for SLH and -4/5 for winds.

Although there is considerable structure in the SLH spectra, there seems to be little difference between seasons. As we can see (Figure II.4, upper panel), the SLH spectrum is red, i.e., more energetic at low frequencies. In both seasons there is a distinctive 14 day peak at all stations, corresponding to the fortnightly component of the tides (M_f). This is a common feature of tropical SLH spectra (see, e.g., Luther, 1980). There are also several peaks at periods shorter than a week. Peaks at the 4.5-4.7 day and 3.5-3.7 day bands are found during both summer and winter seasons. A statistical test shows that there are no significant differences between the summer and winter SLH energy levels (at the 90% level of confidence) in any frequency band. The SLH spectra for the other stations are similar to the one for Talara-Paita. The main difference is found at Buenaventura, where the spectrum is more energetic at all frequencies (3-4 times as large as at the other stations), probably because of the interhemispheric asymmetries in the coastal dynamics, as suggested by Bigg and Gill (1986).

The wind spectra (Figure II.4, lower panel) are less red, i.e.,

rather flat in comparison with the SLH, and there is a tendency to find more energy at frequencies below 0.1 cpd during the winter than during the summer. The wind spectra are less energetic at Lima and Salinas, but a similar pattern is found.

II.4.2 Cross Spectra

Forcing analysis

To determine whether the variability in the SLH series was a response to local winds, we computed the cross spectra between the wind and SLH series at the same locations using the same ensemble-averaging procedures as for the autospectra. In general, the coherence (γ) is not very high at any of the stations, especially at Salinas. We find significant γ^2 peaks at several frequencies but these do not show a consistent pattern between stations. Here we show the cross spectra for Talara-Paita (Figure II.5). During the summer there are narrow peaks of high coherence at 11 days and 8 days, with values that are well above the 90% confidence level. We band averaged the cross spectral estimates in the 8-11 day band (0.091-0.135 cpd) for this season and find that wind forcing explains only one fifth of the SLH variance in this band (γ^2=0.22), although the coherence is significant at the 95% confidence level. The summer coherence at La Libertad and Callao is lower (γ^2=0.15, 0.18) than at Talara-Paita and less significant (90%), and the double peak structure at 8-11 days is not repeated.

The 8-11 day coherence during the winters is somewaht lower (γ^2=0.12, 0.18, 0.11 from north to south) and less significant (80%, 90% and 80%). When we examined individual years, no station had coherence at above the 90% level during more than one of the four seasons, except Talara-Paita (two summers).

In Figure II.5 the phases between Talara-Paita wind and SLH series are plotted as lags in days. Positive lags indicate that wind leads SLH and the plotted curves show the lags corresponding to ±180° phase differences. The phases tend to cluster around ±180° indicating that there is a tendency for sea level to drop when the local wind is stronger (weaker) in the equatorward (poleward) sense, which is the expected local-forcing response. The phase spectra for Salinas-La Libertad and Lima-Callao are similar to the one for Talara-Paita, with the phases tending to group near ±180°. The scatter is greater, however, providing weaker evidence of local forcing (especially at Salinas).

Based on the phase spectra, we conclude that some local forcing probably occurs during the whole year over most of the spectrum, with little difference between summer and winter seasons. From the generally low coherences, however, we infer that locally forced response is relatively weak, i.e., it explains only a small percentage of the total SLH variability. The wind-SLH coherence is most significant in the 8-11 day period range at Talara-Paita during non-ENSO summers, but still explains only a small fraction of the SLH variance.

We also computed the cross spectra between the Talara-Paita and Callao SLH stations and the wind stations immediately to the north, to determine if the forcing is coastal but non-local. The coherence spectra show γ^2 to be very low and not significant at most frequencies. This, plus the fact that the phase spectra show a random distribution of the phases, suggests a total absence of non-local forcing of sea level by the alongshore coastal wind.

Propagation analysis

To see if there was propagation of the SLH fluctuations we computed the cross spectra between adjacent SLH stations. The coherence and phase spectra are shown in Figure II.6 for the case of Talara-Paita vs. Callao. During the summer season γ is significant at the 90% confidence level for periods of 14.0, 9.0, 4.6, 3.7, 3.5 and 2.9 days, and during the winter for periods of 14.0, 7.0, 3.6 and 2.1 days. The high coherences at 14.0 days (M_f tide), 4.6 days and 3.5-3.7 days are found in both seasons. The significant coherences at 9.0 days and 2.9 days appear only during the summer, while those at 7.0 days and 2.1 days appear only during the winter.

Note that during both seasons of non-ENSO years, the 3.5-3.7 day band is the dominant feature; the only signals in or near the 8-11 day band are a weak γ^2 peak at nine days in the summer and a narrow winter peak at seven days. It occurs to us that the 3.5-3.7 day energy may have originated along the equator as locally resonant third mode inertia-gravity waves (Wunsch and Gill, 1976; Luther,

1980) being subsequently transformed into coastal trapped waves at the eastern boundary. The smaller peak at 4.6-4.7 days, also present in both seasons, may similarly correspond to second mode equatorially trapped inertia-gravity waves (see also Chiswell et al, 1987).

The phase spectra for the two seasons differ in that there is a linear dependence of phase on frequency in winter, but not summer. Because we compute the phase spectra between -180 and +180 degrees, propagation appears as a distribution of phases scattered about a set of parallel, sloping lines as we see in Figure II.6 for the winter spectrum (phase wrapping). To determine the linear dependence we compute a simple linear regression with the independent phase estimates weighted by $\gamma^2/(1-\gamma^2)$ (see the discussion by Enfield and Allen, 1983). The winter phase distribution shows the presence of poleward propagating fluctuations with typical speeds of 2.8 ± 0.2 m s^{-1} (95% confidence interval) between Talara-Paita and Callao. This speed is about the same magnitude as those found by Romea and Smith (1983) along the Peru coast between 5°S and 15°S during the 1976-1977 ENSO event. The linear phase-frequency relationship is consistent with non-dispersive coastal trapped Kelvin waves. At the shortest periods (2-3 days) the phases depart from the non-dispersive relation, however. During the summer season there is a weak tendency for the phases to follow a linear distribution at the lowest frequencies, but there is not a clear pattern like the one

found during the winter, therefore is not possible to establish a reliable relationship.

High coherences are found in the cross spectra between La Libertad and Talara-Paita at most frequency bands, especially during the winter season (not shown). The phase distribution at low frequencies (0.011 to 0.120 cpd) indicates that there is some propagation during the winter with a phase speed of approximately 1.8 ± 0.4 m s^{-1} (95% confidence interval); for higher frequencies the phases are widely scattered without any particular pattern.

Theory predicts that equatorial waves incident on the eastern boundary will propagate poleward into both hemispheres as coastal trapped waves. A cross-equatorial analysis between Buenaventura and the coastal stations south of the equator (e.g., La Libertad) would give misleading information about such propagation. However, because we lack data from coastal stations between the equator and Buenaventura we have no way to test for a northern hemisphere propagation.

II.5 FORCING AND PROPAGATION: INTERANNUAL COMPARISONS

II.5.1 Autospectra

To determine the distribution of energy with time as well as with frequency, autospectra were computed for all LLP time series

for successive 250 day segments of data. The data segments are centered at 50 day intervals with a 200 day overlap between segments. Each spectrum was smoothed by applying a running band average with ten degrees of freedom. The log of the spectral density is contoured and shown in Figure II.7 for the Talara-Paita SLH series. As shown in Figure II.4 (top), the spectrum is red, i.e., more energy is found at low frequencies. During the 1982-1983 ENSO episode there is an increase in energy level at most of the frequency bands. In particular, there is a dramatic, tenfold increase of the variance in the 0.09 to 0.13 cpd frequency band, which corresponds to periods of 8 to 11 days, consistent with the statistical tests applied to the residual series (Table II.2). We find a similar pattern repeated at other coastal stations. Santa Cruz, however, shows an increase of energy level only at very low frequencies (less than 0.06 cpd).

Based on the statistics of the SLH series (Table II.2), we have defined three 13-month periods, each bracketing the 1982-1983 ENSO event. These periods are defined as follows: pre-ENSO, from June 1981 to June 1982; ENSO, from September 1982 to September 1983; and post-ENSO, from December 1983 to December 1984. The rms amplitudes of the series segments (Table II.3) are equal to the square root of the 8-11 day band variance, which is computed as the spectral density times the bandwidth. The comparisons show that the pre- and post-ENSO periods are significantly different from the ENSO segment at the 99% confidence level at La Libertad, Talara-Paita and Callao.

The amplitudes during the ENSO episode were at least twice as large as before or after the El Niño for all the coastal stations south of the equator (see Table II.3). At Talara-Paita the variance ratio (from Table II.3) between the ENSO and non-ENSO periods is 10.4, consistent with the order of magnitude increase in spectral energy noted in Figure II.7. The ENSO variability at Santa Cruz is also greater, but is different from the non-ENSO period only at the 75% confidence level.

The autospectra for the wind series (not shown) do not have any salient features. Statistical tests between the different periods show a small increase of the rms amplitudes of the LLP series that is significant only at the 90% confidence level at Talara and Salinas when the ENSO period was compared with the pre- and post-ENSO ones. Differences at Lima (decrease in the rms amplitudes) were only significant at the 75% confidence level.

We also observe a ridge in the SLH autospectra around 0.07 cpd which corresponds to the M_f component of the tides. It is poorly defined in Figure II.7 due to the blurring effect of the coarse bandwidth on the narrow peak. Its energy remains nearly constant during the six year period analyzed (1979-1984). The energy increase observed in the 8-11 day band during ENSO also extends to higher frequencies, and is especially evident in the 0.17-0.25 cpd frequency range. This increase at higher frequencies may correspond to the coastal extension of incident, equatorial inertia-gravity waves at periods of 4-6 days, noted previously in the alongshore

coherence spectra (Figure II.6).

II.5.2 Cross Spectra

Forcing analysis

To determine if the energetic SLH fluctuations during the 1982-1983 ENSO episode were a response to the local wind, the cross spectra were computed between the LLP wind and SLH series at each station and for each of the three periods: pre-ENSO, ENSO and post-ENSO. Figure II.8 shows the results for Talara-Paita, which has the strongest wind variability and showed the clearest evidence for local forcing in the seasonal analysis. The results for Salinas-La Libertad and Lima-Callao are wholly consistent with those for Talara-Paita.

The coherence is generally low before and after the event, with some significant values at frequency bands that are not repeated for either period. Except at the longest periods (three weeks or longer), the ENSO episode has the least coherent forcing spectrum, especially near 8-11 days. Significant γ^2 values (99% confidence level) are found near this band before (8.5 days) and after (11.4 days) the ENSO event, but are uniformly small over the same range during ENSO.

Although the coherence is generally low, the phase estimates tend to aggregate near $\pm 180^\circ$ and thus indicate a weak local forcing, as for the non-ENSO seasons. The robustness of phase estimates in

the presence of incoherent noise has been noted by Schott and Düing (1976), who point out that autospectral estimates do not contribute noise to the phase computations, as they do in the calculation of coherence. We interpret the low coherence in the presence of local wind forcing to mean that a large component of the SLH variability consists of random noise and remotely forced propagating signals.

Propagation analysis

To explore the alongshore propagation characteristics, we computed the cross spectra between adjacent SLH stations for each of the three periods. In Figure II.9 we show the results for Talara-Paita vs Callao. The coherence is noticeably higher during the ENSO period, especially in the 8-11 day band, while for the pre- and post-ENSO periods the coherence in the 8-11 day band is low or not significant. The coherence in this range is significant in several narrower frequency bands, but without a common pattern between the two periods. Interestingly, the M_f band is coherent both before and after, but not during the ENSO event. There are significant γ^2 peaks in higher frequency bands that may correspond to resonant inertia-gravity waves along the equator. The coherences are much higher in the 4.6-4.7 day and 3.5-3.7 day bands during the ENSO event than either before or after. This is also consistent with the higher energy found during ENSO at the higher frequencies (Figure II.7).

For the ENSO period the phase distribution is similar to the

one found for the non-ENSO winter seasons (Figure II.6). The linear distribution of phase shows a very well defined poleward, nondispersive propagation at all frequencies where $\gamma^2>0.21$ (80% confidence) and is an indicator of the presence of coastal trapped waves. After applying a linear regression fit (with independent phase estimates weighted by $\gamma^2/(1-\gamma^2)$) we find that the variability is propagating poleward with an overall phase speed of 3.5 ± 0.1 m s^{-1} (95% confidence interval). This propagation is much faster than the value of 2.8 m s^{-1} found in our analysis of the non-ENSO winters. The phase distributions for the other periods do not show a clear propagation pattern. There is some suggestion of a similar propagation prior to the ENSO at lower frequencies (0.011-0.20 cpd), but we are unable to find a linear relationship with any confidence.

The strong alongshore coherence of sea level in the 8-11 day band during the 1982-1983 El Niño stands in sharp contrast to the lack of coherence between sea level and local winds at that time. This is strong confirmation that the propagating variability is not locally forced; its presence decreaes, rather than enhances, the wind-SLH coherence.

The cross spectrum between La Libertad and Talara-Paita (not shown) also shows highly significant coherence (over the 99% confidence) in the 8-11 day band during the ENSO period. For higher frequencies the coherence is very low or not significant. The distribution of the phases in the 0.011 to 0.150 cpd range indicates

poleward propagation of signals with speeds of 1.8±0.3 m s^{-1} (95% confidence interval) which is similar to the value found in our seasonal analysis. For higher frequencies the phases do not follow a specific pattern. It is difficult to ascertain what phase speed we should expect between La Libertad and Talara-Paita, because this station pair lies partially within the equatorial waveguide. For the pre-ENSO and post-ENSO periods the coherences are not significant in the 8-11 day band and the phase spectra do not show propagation at all.

II.6 SUMMARY AND DISCUSSION

The major goal of this work was to determine the seasonal and interannual changes in the characteristics of high frequency (days-weeks) variability in the sea level along the west coast of South America, namely, its forcing and propagation. To accomplish this we have compared wind-SLH relationships and alongshore SLH structures between Austral summer and winter seasons for normal (non-ENSO) years and interannual periods (ENSO and non-ENSO years).

Comparisons between seasons have shown that there are no significant differences between summer and winter energy levels in either the SLH or wind series. Studies of the annual cycle of the sea level in the eastern tropical Pacific by Bigg and Gill (1986) have shown that the coastal sea level has two components: 1) the

local response to the wind, and 2) the remotely forced one. At much higher frequencies, we find evidence from phase spectra of a weak local forcing at all stations, but it is responsible for only a small percentage of the total variance in the sea level. Most of the variability is spatially incoherent noise or is remotely forced. In particular, the cross spectrum between wind and SLH series at Salinas-La Libertad, closer to the equator than previous studies have examined, shows much less evidence of local forcing by the alongshore wind than at Talara or Callao.

The auto- and cross spectra of SLH have revealed the presence of energy in the 3.5-3.7 and 4.6-4.7 day bands. The signals in these bands were stronger during the 1982-1983 ENSO than either before or after the event. These peaks may correspond to second and third mode, locally resonant inertia-gravity waves along the equator, such as have been observed previously by Wunsch and Gill (1976) and Luther (1980) in the sea level records of islands near the equator. This possibility is supported by the fact that Chiswell et al (1987) found evidence in the spectra from inverted echo sounders in the eastern equatorial Pacific for the second and third mode inertia-gravity waves in 1982-1983.

The most important difference between summer and winter seasons is found in the phase spectra computed between adjacent SLH stations. A clear alongshore phase propagation is evident during the Austral winters but not during the summers. The poleward propagation of 2.6-3.0 ms^{-1} between Talara-Paita and Callao (Figure

II.6), at periods of 2-30 days, is consistent with baroclinic coastal trapped waves previously observed along the Peru coast. The fact that SLH is unforced by remote coastal winds to the north (Section II.4.2) indicates that these propagating fluctuations were not coherent with the wind anywhere along the coast.

The interannual comparisons of forcing and propagation indicate that the energy, alongshore coherence, and phase propagation (3.4-3.6 m s^{-1}) were strongly developed during the 1982-1983 ENSO along the Ecuador-Peru coast. A weak, locally forced response in coastal sea level always occurs, but is obscured because noise and remotely forced variability overwhelm estimates of coherence between wind and sea level. This conclusion is based mainly on the wind-SLH phase relationship. It constitutes a clarification, not a contradiction of previous studies (Smith 1978, Brink 1982, Romea and Smith 1983), which have called attention to the ubiquitous propagating variability found along the Peru coast while noting that sea level is <u>incoherent</u> with the local alongshore winds. The high alongshore coherence between sea level stations in the 8-11 day band and the lack of coherence between wind and sea level series in the same band clearly indicate that the strong SLH fluctuations were remotely forced during the 1982-1983 ENSO.

The fact that the coastal fluctuations were traveling 1.4 times faster during the latest event (~3.5 ms^{-}) than during the non-ENSO winter seasons (~2.8 ms^{-1}) is significant. Brink (1982) has shown that between Talara-Paita and Callao the topography and

stratification are important factors in determining the structure and behavior of coastally trapped waves. The topography, of course, is temporally invariant. However, changes in the stratification seem to have been more intense between Talara-Paita and Callao, along the Peru coast, during the 1982-1983 ENSO than during the winter seasons. These changes may be sufficient to account for the difference in the propagation speeds. If we use a two-layer system to model the coastal fluctuations ($c=\sqrt{gH}$, $g=9.8$ m s^{-2}, H=equivalent depth) and the phase speeds (c) determined by the alongshore cross spectra for both periods, 2.8 m s^{-1} (non-ENSO winters) and 3.5 m s^{-1} (1982-1983 ENSO), we find that the equivalent depth H is about 60% greater during the 1982-1983 ENSO (H= 1.25 m) than during the non-ENSO periods (H= 0.80 m). These results are consistent with the descriptive analysis by Leetmaa et al (1987) of CTD sections across the equator along 85°W, and along 5°S and 10°30'S between 85°W and the South American coast, before, during and after the 1982-1983 ENSO event. They find that the thermocline, generally represented by the 15°C isotherm, was considerably deeper during the 1982-1983 ENSO than either before or after the event. The anomalous depression of the 15°C isotherm was approximately 70% of the non-ENSO depth. Therefore, the changes in propagation speeds between non-ENSO winters and the 1982-1983 ENSO are quantitatively consistent with the observed changes in the stratification.

The increase of the variance in the 8-11 day band at the coastal stations, the near absence of this signal at Santa Cruz

(near equator) and the results presented by Chiswell et al seem to indicate that the 1-2 week coastal variability during the 1982-1983 ENSO may be primarily to the arrival of energy in the form of equatorially trapped Yanai waves. In a companion study (Enfield et al, 1987), we combine equatorial and coastal data to identify the equatorial origin of the observed propagating variability along the coast. In addition, we feel that a search for the ultimate source of the wave energy and the reasons for its extraordinary intensity during the El Niño should be attempted.

II.7 CONCLUSIONS

We have studied the characteristics of high (5-7 days to 3-4 weeks) frequency sea level and wind variability along the west coast of South America. The principal results of this study can be summarized as follows:

1. There are no significant differences in the energy levels of winds and sea level between Austral summers and winters

2. There is some evidence for a weak, locally forced response at all stations. The locally forced variability, however, is responsible for only a small fraction of the SLH variance, although it occurs for both seasons and for both ENSO and non-ENSO periods.

3. During the winter seasons there is poleward propagation of SLH coastal fluctuations at speeds of 2.8 ms^{-1} between Talara-Paita and Callao, consistent with previous evidence of low mode coastal

trapped waves along the Peru coast.

4. The autospectra for multi-year SLH series shows a tenfold increase of the variance in the 8-11 day band during the 1982-1983 ENSO event at all coastal stations. The signal is unforced along the coast and is characterized by strong alongshore coherence and a poleward phase speed of 3.5 ms^{-1} , consistent with an anomalous depression of the coastal density structure during the 1982-1983 ENSO.

Table II.1- Given for each station is its name, abbreviation, location and data source, follow by the name and data source for the local wind station if any. Data sources are: University of Hawaii (UH), Instituto Oceanografico de la Armada del Ecuador (INOCAR), Direccion de Hidrografia y Navegacion de la Marina del Peru (DHNM), Corporacion de Aviacion Civil del Peru (CORPAC) the Instituto Geografico Agustin Codazzi de Colombia (IGAC) and the National Oceanic and Atmospheric Administration's Equatorial Pacific Ocean Climate Studies (EPOCS) program. The Talara and Paita sea level series have been combined (see text) and referred to as Talara-Paita (TPA).

Sea level Station	Abbr	Lat	Lon	Source	Wind Station	Source
Buenaventura	BVA	3°54'N	77°05'W	IGAC	none	none
La Libertad	LLB	2°12'S	80°55'W	INOCAR	Salinas	INOCAR
Santa Cruz	STZ	0°45'S	90°18'W	UH	none	none
Talara	TPA	4°37'S	81°17'W	DHNM	Talara	CORPAC
Paita		5°05'S	81°07'W	EPOCS	none	none
Callao	CAL	12°03'S	77°09'W	DHNM	Lima	CORPAC

Table II.2 Ratios (ENSO/non-ENSO) of the rms amplitudes of the residual SLH series. Ratios greater than 1.40, 1.55 and 1.88 are significant at 90%, 95% and 99% confidence levels, respectively. Station abbreviations are defined in Table II.1.

Station	ENSO/Pre-ENSO	ENSO/Post-ENSO
BVA	1.25	1.31
LLB	2.50	2.24
STZ	1.49	1.33
TPA	3.41	4.03
CAL	2.65	2.38

Table II.3 Rms amplitudes of the SLH time series in the 8-11 day band before, during and after the 1982-1983 El Niño. Sea level differences greater than 1.40, 1.55 and 1.88 are significant with 90%, 95% and 99% confidence levels, respectively. Station abbreviations are defined in Table II.1.

Station	Pre-ENSO	ENSO	Post-ENSO
BVA	2.77	4.50	3.37
LLB	2.08	4.63	2.12
STZ	1.43	1.94	1.68
TPA	1.36	4.31	1.30
CAL	1.59	3.41	1.69

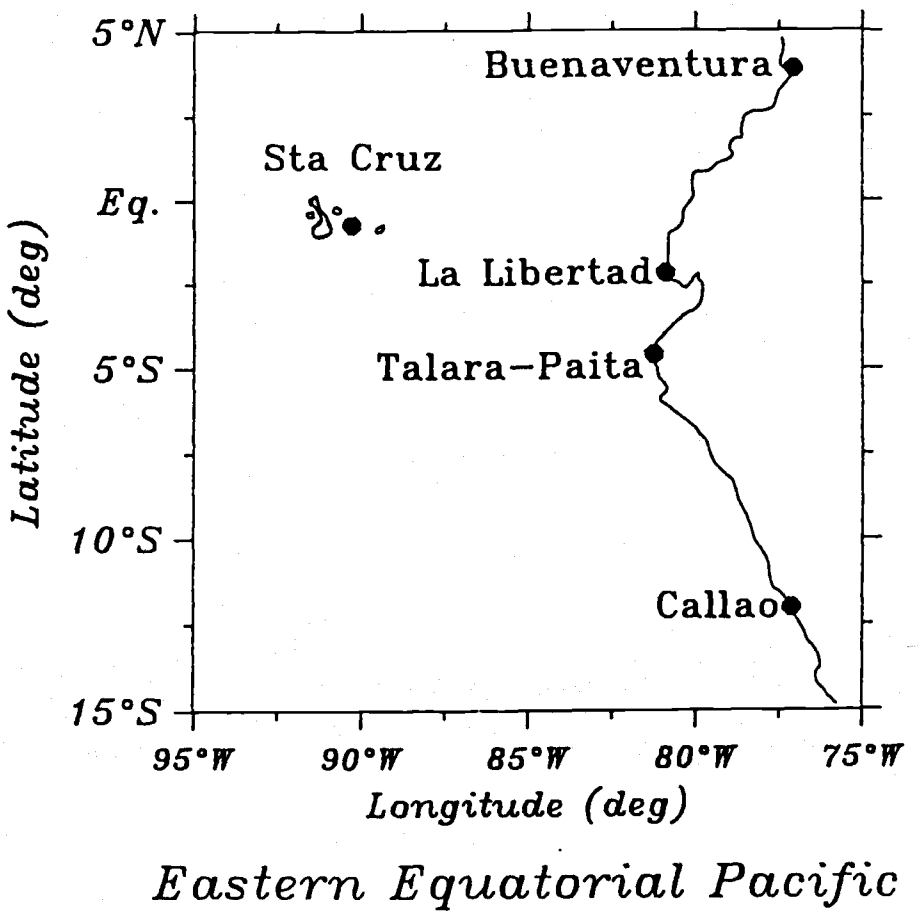

Figure II.1 Locations of sea level stations stations in the eastern equatorial Pacific.

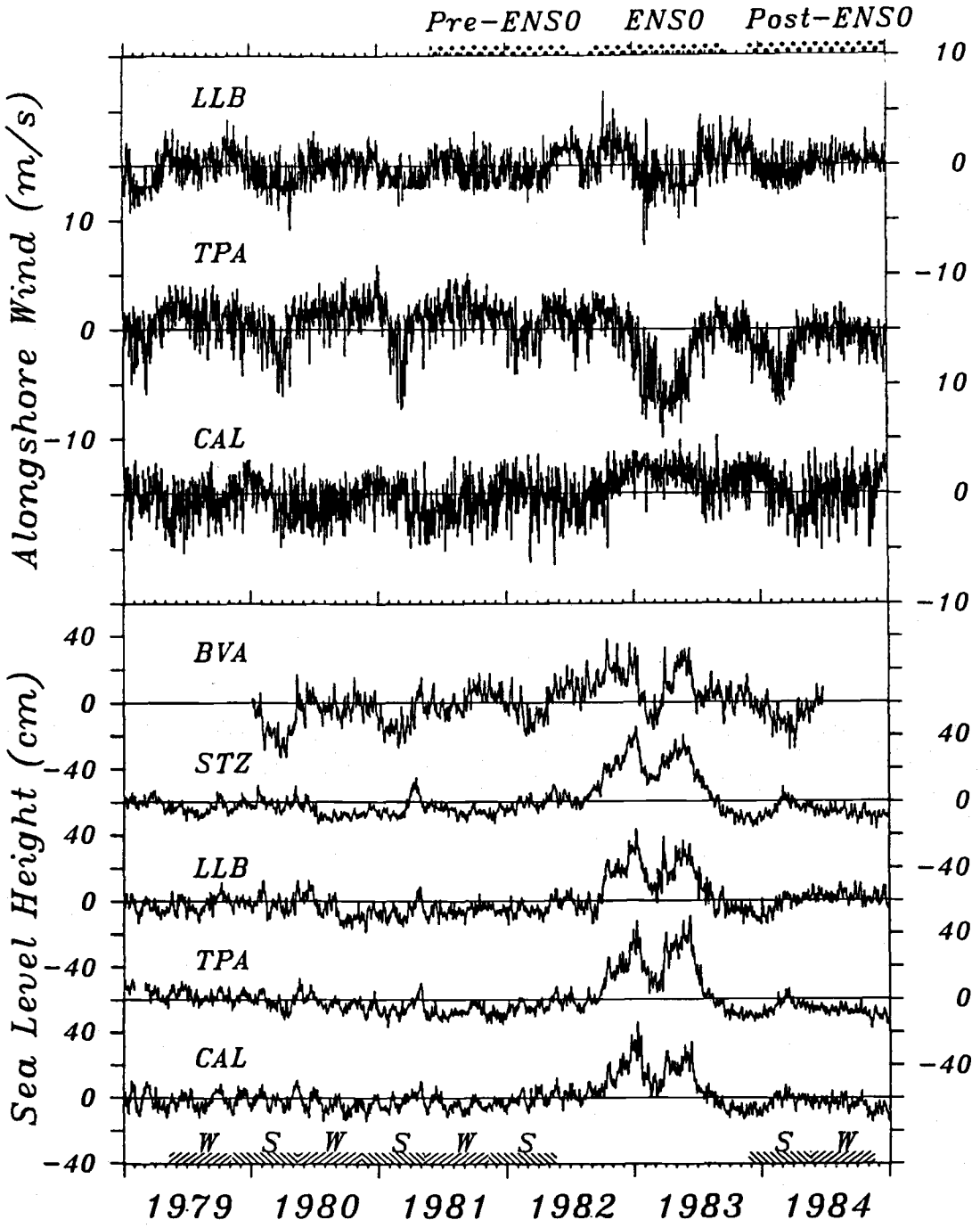

Figure II.2 Time series of LLP filtered SLH and wind data. Upper panel is for the alongshore component of the wind. Lower panel is for the sea level data. The temporal distribution of the seasonal periods is shown along the lower time axis for summers (S) and winters (W). The pre-ENSO, ENSO and post-ENSO periods are shown along the upper time axis. Station abbreviations are defined in Table II.1.

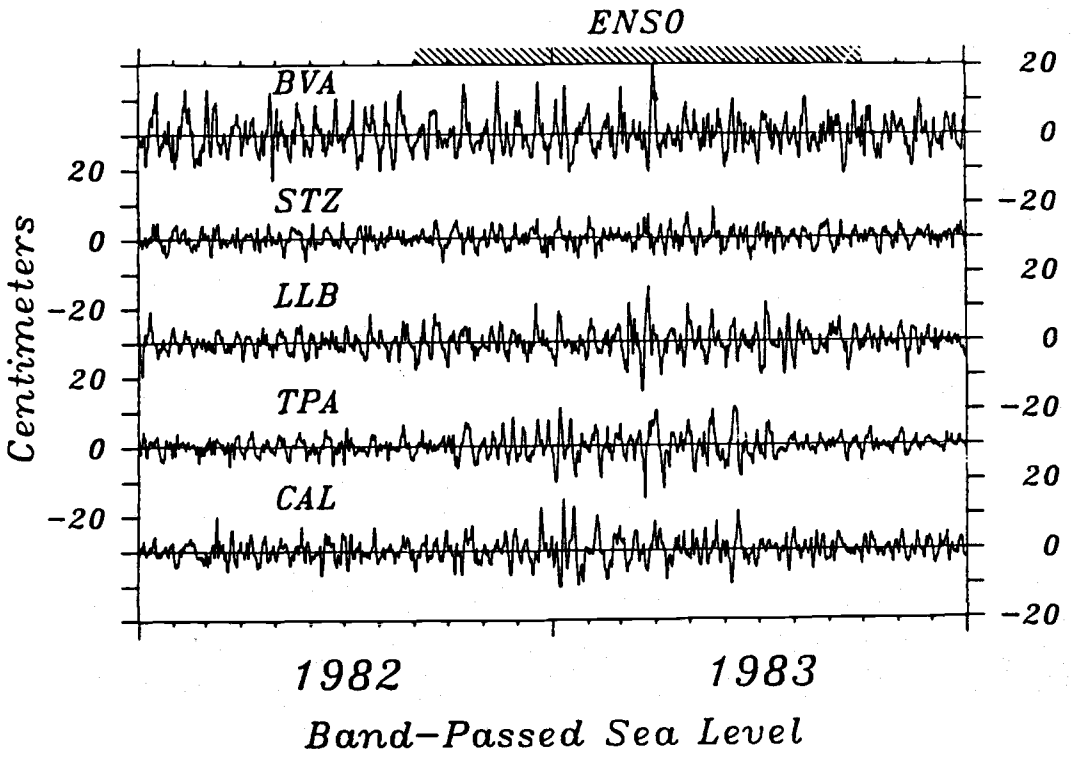

Figure II.3 Band-passed series of sea level. Note the increased amplitudes of the 1-2 week fluctuations during the 1982-1983 ENSO, which are most evident at the coastal stations in Ecuador and Peru but not at Santa Cruz near the equator.

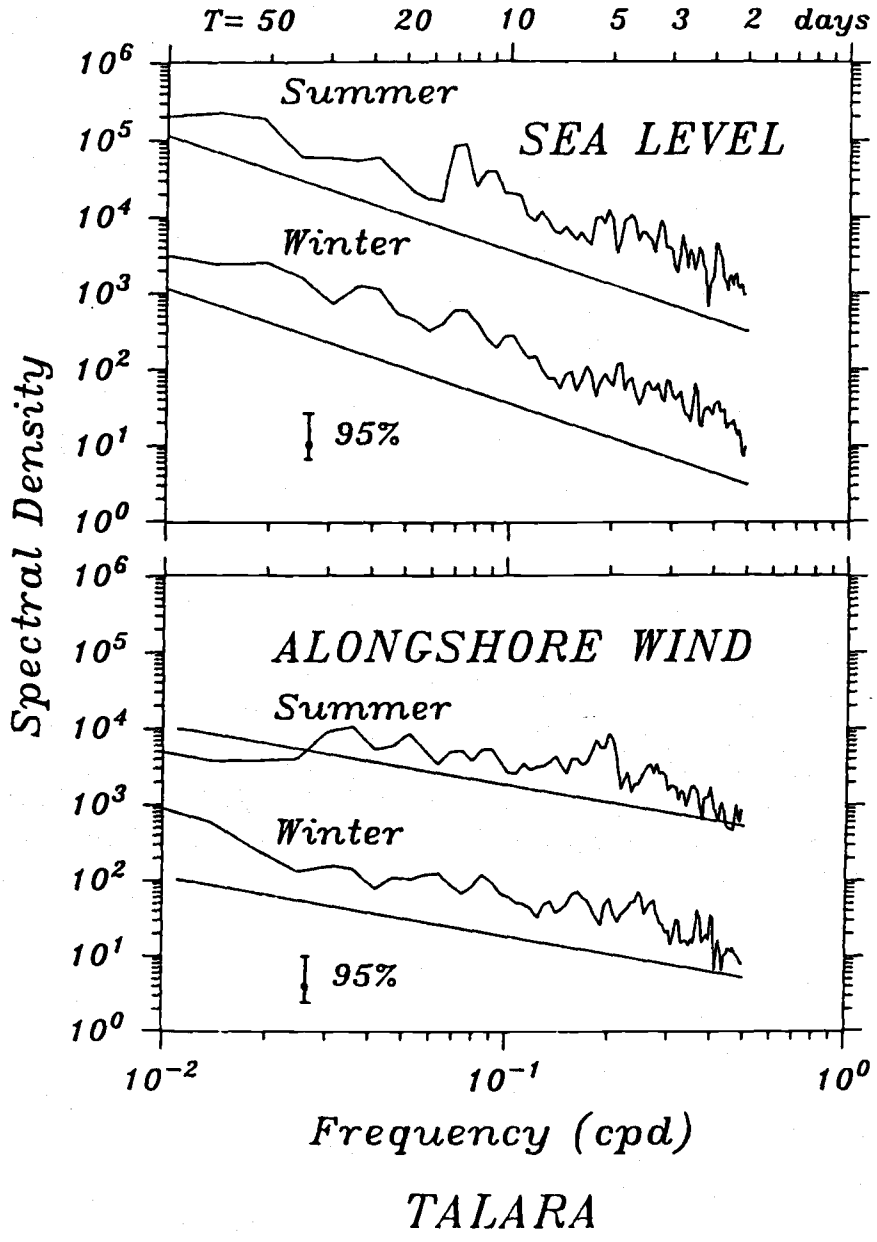

Figure II.4 Autospectra for non-ENSO summers and winters at Talara. Upper panel is for SLH series and lower panel for wind series. Spectral density units are cm^2/cpd for sea level and $(m\ s^{-1})^2/cpd$ for wind. Periods (T) in days are shown at the top.

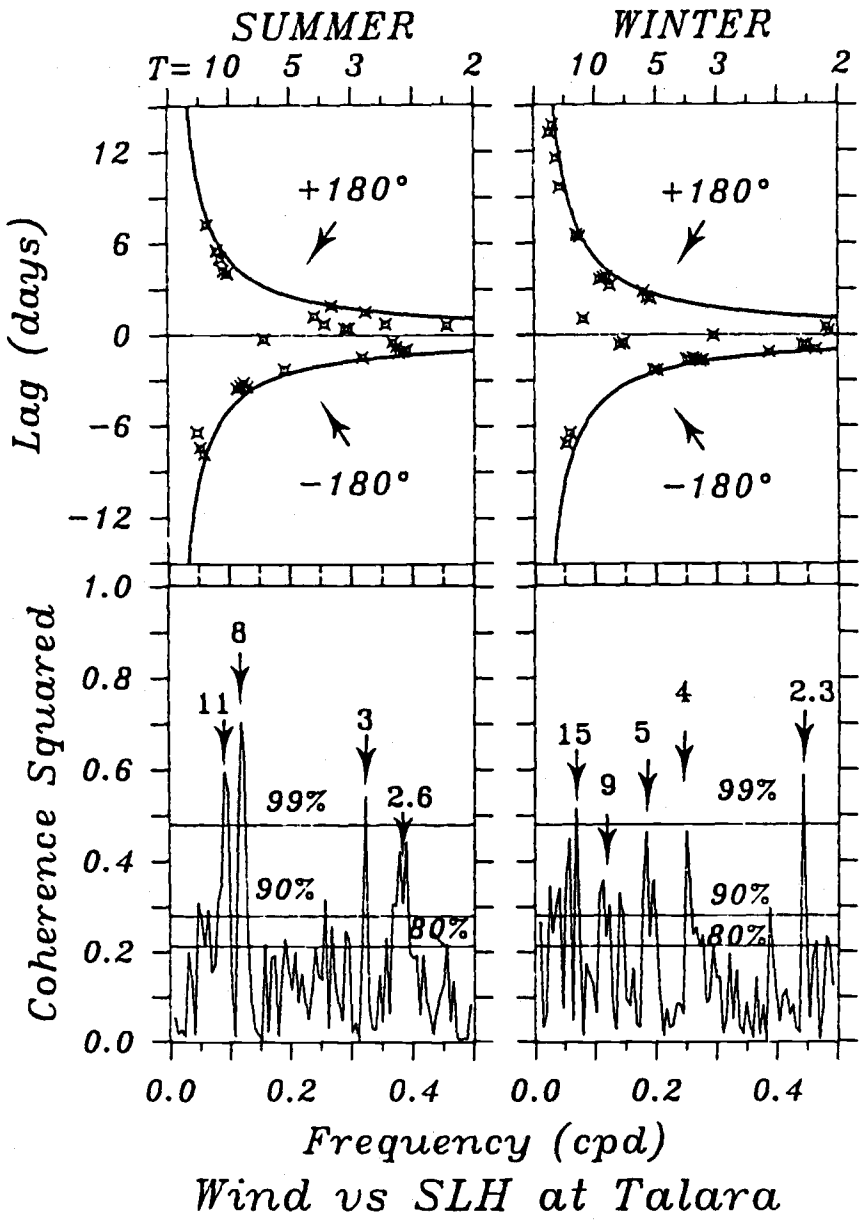

Figure II.5 Cross spectra between wind and SLH series at Talara for the Austral summer (left panels) and winter (right panels). The upper panels show the distribution of lags (days) with frequency ($\gamma^2 \geq$ 80% confidence level). The periods (T) in days are shown at the top. The lower panels show the corresponding coherence spectra and their 80%, 90% and 99% significance levels. Periods of coherence peaks are also shown.

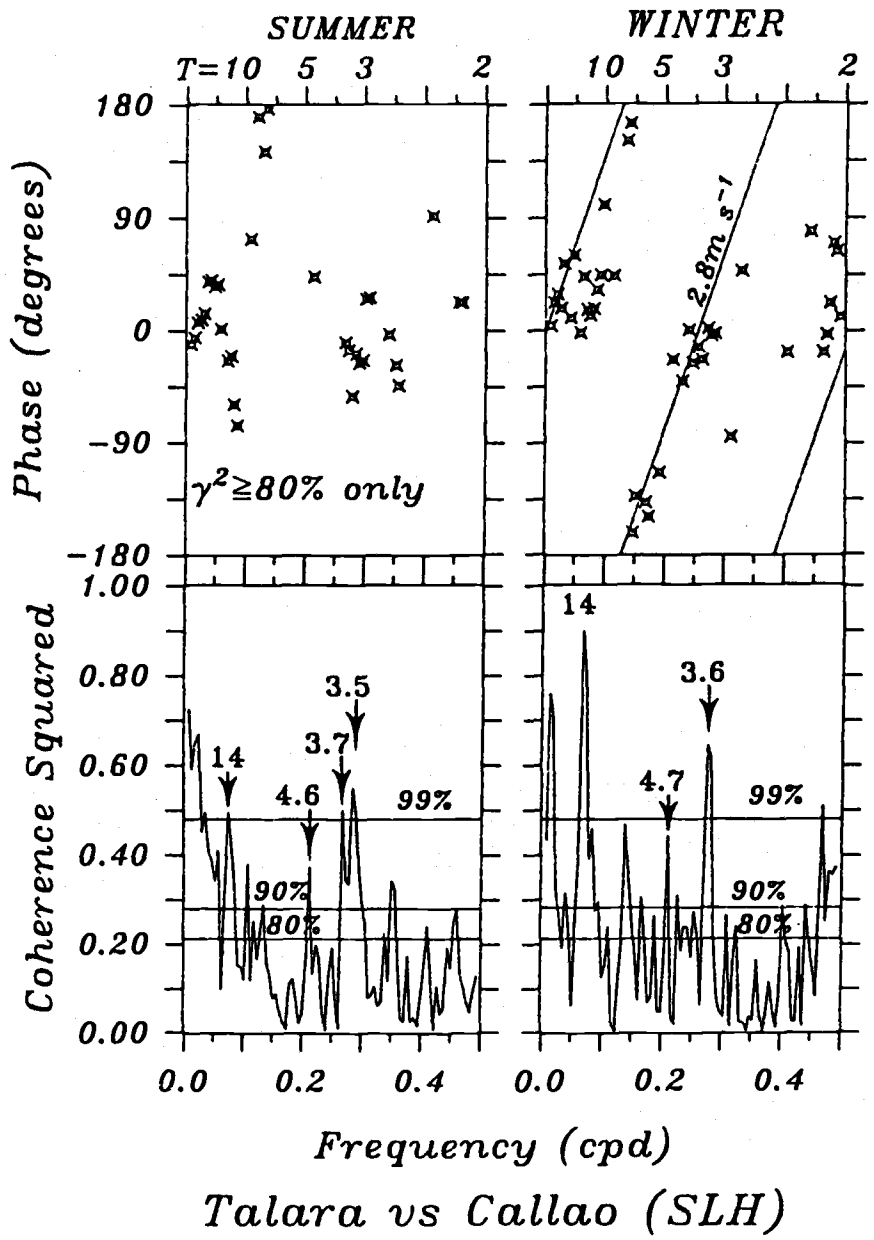

Figure II.6 Cross spectra between Talara-Paita and Callao. The left (right) panels show the cross spectrum for summer (winter). Tilted lines on the phase spectra are the weighted least squares linear fits constrained to pass through the origin. Periods (T) in days are shown at the top. Periods of coherence peaks are also shown.

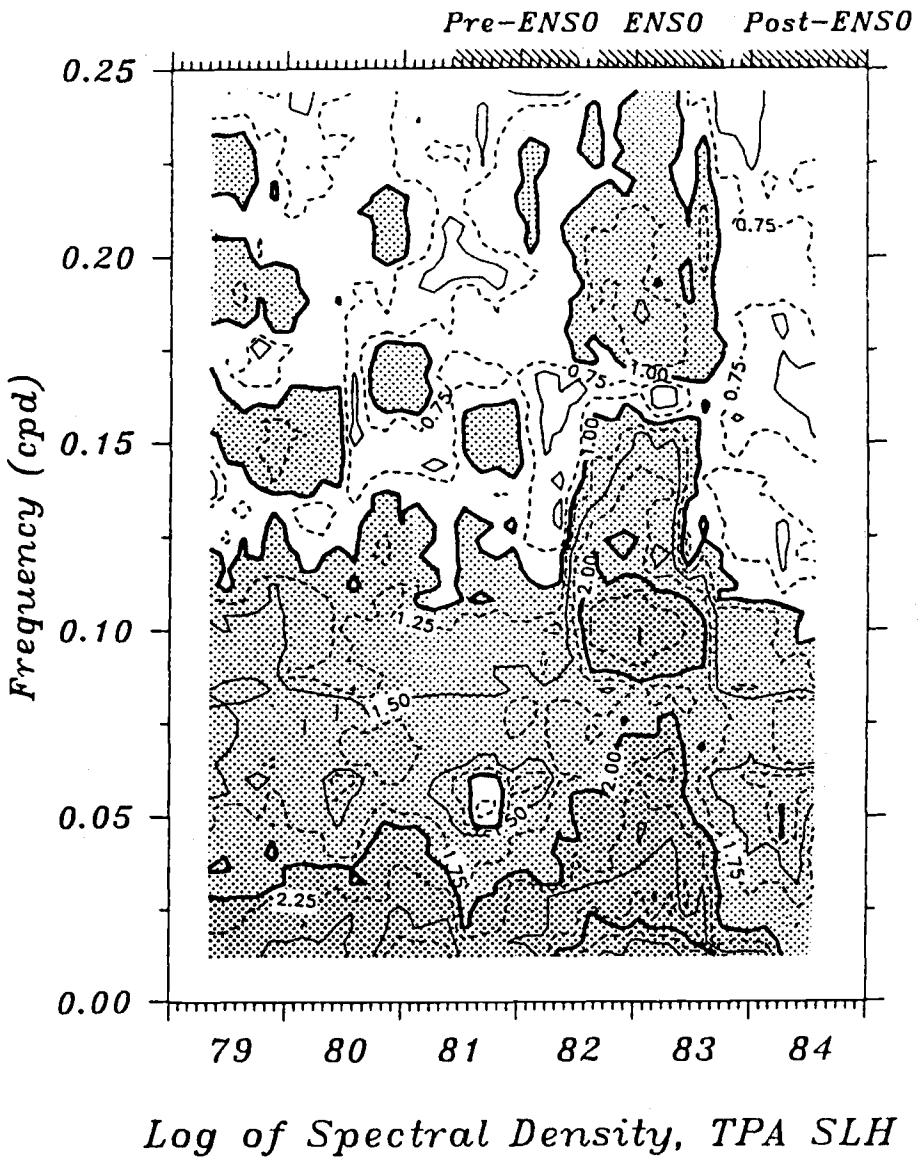

Figure II.7 Contour plot of the log of spectral density (cm^2/cpd) as a function of time and frequency for the SLH series at Talara-Paita. The chance probability that a feature lies more than 0.26 above a given value is less than 10%. Dark (light) shading indicates log values above 2.0 (1.0). The temporal distribution of the interannual periods is shown on the upper time axis.

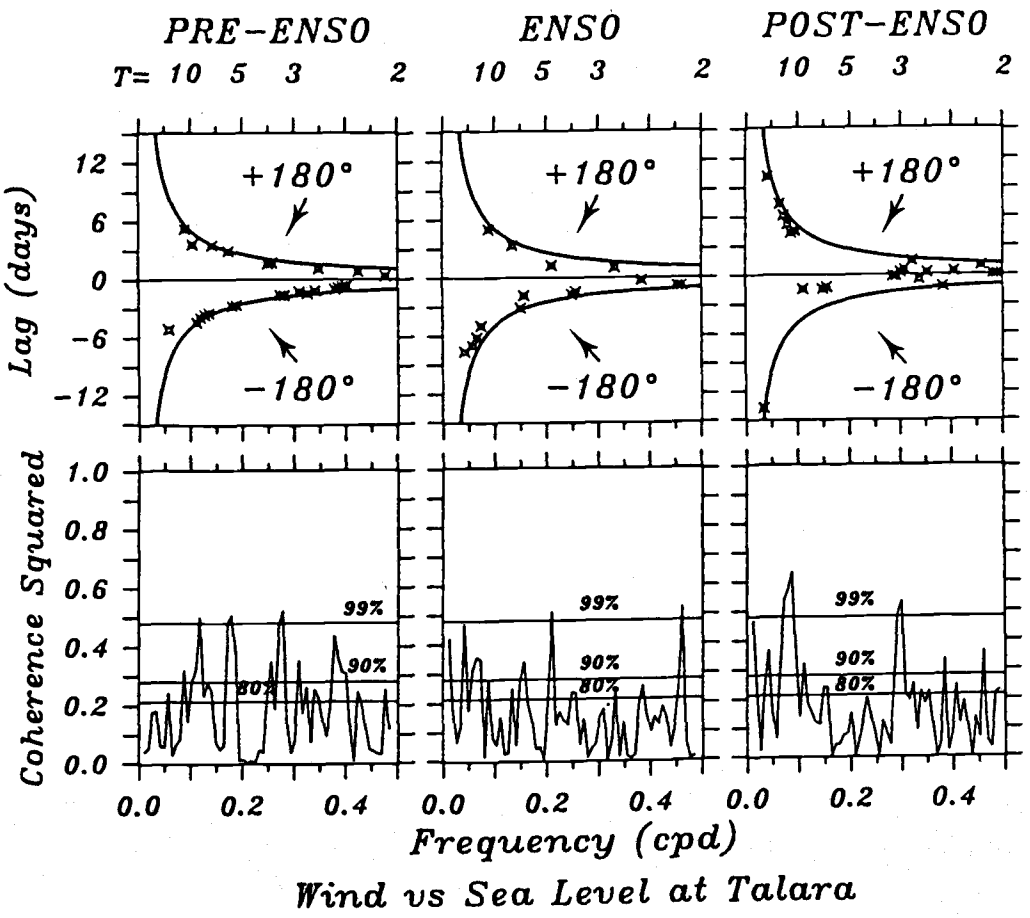

Figure II.8 Cross spectra between wind and SLH series at Talara-Paita for the interannual periods. Calculations are done for the three 13-month periods, using running band averages with five overlapping frequencies yielding 16 df and a bandwidth of 0.0203 cpd. The upper panels show the lag distributiuon with frequency ($\gamma^2 \geq 80\%$ confidence level). The curved lines show the expected local-forcing response (as in Figure II.5). The lower panels show the corresponding coherence spectra. Periods (T) in days are shown at the top.

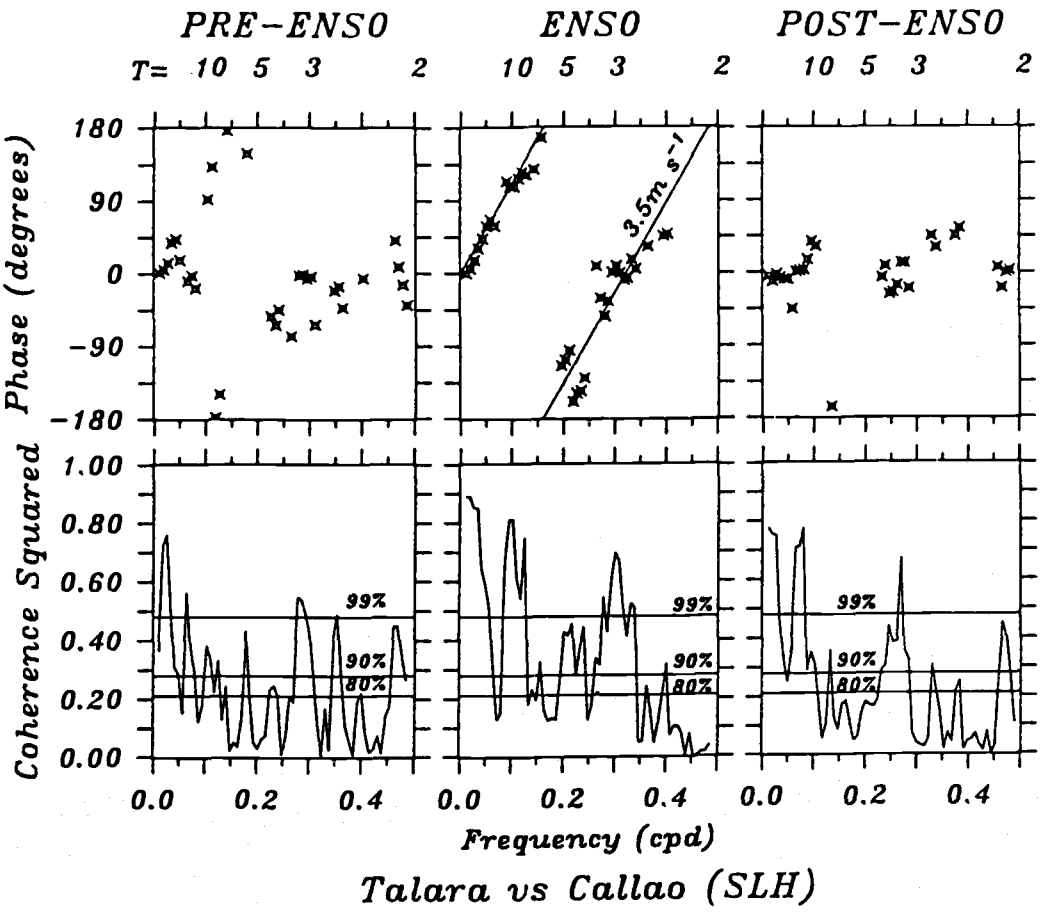

Figure II.9 Cross spectra between Talara-Paita and Callao for the interannual periods. The calculations are done as for Figure II.8. The upper panels show the phase spectra. The sloping lines in the phase spectra are the weighted least squares linear fit, constrained to pass through the origin. The lower panels show the corresponding coherence spectra. Periods (T) in days are shown at the top.

REFERENCES

Allen, J.S. and R.D. Romea, On coastal trapped waves at low latitudes in a stratified ocean, J. Fluid Mech., 98, 555-585, 1980.

Bigg, G.R. and A.E. Gill, The annual cycle of sea level in the eastern tropical Pacific, J. Phys. Oceanogr., 16, 1055-1061, 1986.

Brink,K.H., A comparison of long coastal trapped wave theory with observations off Peru, J. Phys. Oceanogr., 12, 897-913, 1982.

-----, J.S. Allen and R.L. Smith, A study of low frequency fluctuations near the Peru coast, J. Phys. Oceanogr., 8, 1025-1041, 1978.

Chiswell, S.M., D.R. Watts and M. Wimbush, Inverted echo sounder observations of zonal and meridional dynamic height variability in the eastern equatorial Pacific during the 1982-83 El Niño. Deep Sea Res., in press, 1987.

Clarke, A.J., The reflection of equatorial waves from oceanic boundaries, J. Phys. Oceanogr., 13, 1193-1207, 1983.

Enfield, D.B., Thermally driven wind variability in the planetary boundary layer above Lima, Peru, J. Geophys. Res., 86, 2005-2016, 1981a.

-------, Annual and non-seasonal variability of monthly low-level wind fields over the southeastern tropical Pacific, Mon. Wea. Rev., 109, 2177-2190, 1981b.

-------, and J.S. Allen, On the structure and dynamics of monthly mean sea level anomalies along the Pacific coast of North and South America, J. Phys. Oceanogr., 10, 557-578, 1980.

-------,and ------, The generation and propagation of sea level variability along the Pacific coast of Mexico, J. Phys.Oceanogr., 13, 1012-1033, 1983.

-------, M.P. Cornejo-Rodriguez and R.L. Smith, On the source of 8-11 day propagating signals in the coastal sea level off South

America during the 1982-1983 El Niño, submitted to J. Geophys. Res., 1987.

--------, and P.A. Newberger, Peru coastal winds in 1982-83, Proceedings of the Ninth Annual Climate Diagnostic Workshop, Oregon State University, 22-26 October 1984. U.S. Dept. of Commerce, National Oceanic and Atmospheric Administration, pp. 147-156, 1984.

Hayes, S.P. and D. Halpern, Correlation of current and sea level in the eastern equatorial Pacific, J. Phys. Oceanogr., 14, 811-824, 1984.

Leetmaa, A., D.W. Behringer, A. Huyer, R.L. Smith and J. Toole, Hydrographic conditions in the eastern Pacific before, during and after the 1982/83 El Niño, submitted to Prog. Oceanogr., 1987.

Lukas, R., S.P. Hayes and K. Wyrtki, Equatorial sea level response during the 1982-83 El Niño, J. Geophys. Res., 89, 10,425-10,430, 1984.

Luther, D.S., Observations of long period waves in the tropical oceans and atmosphere, Ph. D. Thesis, Massachusetts Institute of Technology-Woods Hole Oceanographic Institution, February 1980, 210 pp.

Mangum, L.J. and S.P. Hayes, The vertical structure of the zonal pressure gradient in the eastern equatorial Pacific, J. Geophys.Res., 89, 10,441-10,449, 1984.

Moore, D.W., Planetary-gravity waves in an equatorial ocean, Ph. D. Thesis, Harvard University, 1968, 207 pp.

Romea, R.D. and R.L. Smith, Further evidence for coastal trapped waves along the Peru coast. J. Phys. Oceanogr., 13, 1341-1356, 1983.

Schott, F. and W. Düing, Continental shelf waves in the Florida straits, J. Phys. Oceanogr, 6, 451-460, 1976.

Smith, R.L., Poleward propagating perturbations in currents and sea levels along the Peru coast. J. Geophys. Res., 83, 379-391, 1978.

White, W.B., G.A. Meyers, J.R. Donguy and S.E. Pazan, Short-term climatic variability in the thermal structure of the Pacific ocean during 1979-82, J. Phys. Oceanogr., 15, 917-935, 1985.

Wunsch, C. and A.E. Gill, Observations of equatorially trapped waves in Pacific sea level variations, Deep-Sea Res., 23, 371-390, 1976.

Wyrtki, K., The slope of sea level along the equator during the 1982/1983 El Niño, J. Geophys. Res., 89, 10,419-10,424, 1984.

CHAPTER III

EQUATORIAL SOURCE OF THE PROPAGATING VARIABILITY ALONG THE PERU COAST

ABSTRACT

Using data we have obtained from tide gauges in South America and an array of pressure gauges and inverted echo sounders within and around the Galapagos archipelago, we have analyzed the equatorial origin of coastal trapped waves observed along the Peru coast during the intense 1982-1983 El Niño. It was shown by Cornejo-Rodriguez and Enfield (1987) that the propagating fluctuations along the coast were much stronger at that time than either before or after the El Niño, and that the variability was not locally forced by coastal winds. We find that strong coastal variability was also more energetic during previous El Niño ocurrences. Separating the equatorial surface displacement series into their meridionally symmetric and antisymmetric components, we find that the antisymmetric variability dominated the eastern equatorial zone in the 1-2 week period band. The meridional and zonal phase structure of the displacement data, as well as their amplitude distribution, establish the equatorial fluctuations as mixed Rossby-gravity (Yanai) waves having zero wavenumber near 10

days and standing wave characteristics in the 8-11 day band, in agreement with theory. They were the principal source of the strong trapped wave variability along the Ecuador-Peru coast during the latest El Niño episode. The ultimate source of the Yanai waves and the reason for their intensity during El Niño periods are subjects for future research.

III.1 INTRODUCTION

The objective of this study is to finally answer a question that has perplexed oceanographers for some time: Does the 1-2 week period propagating variability observed along the Peru coast originate in the equatorial waveguide? If so, what is the dominant form of equatorial variability that affects the coast?

Poleward propagating fluctuations in the 1-2 week period band have been detected in sea level along the Peru coast during the El Niño events of 1976-1977 (Smith, 1978; Brink et al 1978; Brink, 1982; Romea and Smith, 1983) and 1982-1983 (Cornejo-Rodriguez and Enfield, 1987). The propagating fluctuations are incoherent with the alongshore coastal winds and the characteristics of the variability are consistent with those of freely propagating, first baroclinic mode coastal trapped waves (Brink, 1982).

Romea and Smith (1983) have analyzed the 1976-1977 currents and sea level fluctuations in the 0.1-0.2 day^{-1} (cpd) frequency band along the Peru coast (5°S-15°S). They find poleward propagating fluctuations with phase speeds of 2-3 m s^{-1} which were not locally forced, but they lacked the data to check the possibility of coastal forcing north of 5°S. They tried to establish a link between the coastal fluctuations in the days-weeks band and equatorial variability by comparing one tide station in the Galapagos Islands

(Baltra Island, 27 nm south of the equator) with the stations along the Peru coast. They found only tenuous evidence to support equatorially trapped Kelvin waves as the source for the coastal propagating signals.

Cornejo-Rodriguez and Enfield (1987) have analyzed sea level and wind series from stations in the eastern equatorial Pacific for the 1979-1984 period. They find a dramatic increase in sea level energy levels in the 8-11 day band during the 1982-1983 El Niño/Southern Oscillation (ENSO) at coastal stations (Figure III.1) but not at Santa Cruz (near equator). They show that the strong, poleward propagating coastal signals in the 8-11 day band were superimposed on a weaker, locally forced variability. They also note that the absence of signal in the 8-11 day band at Santa Cruz was consistent with the antisymmetric sea level structure of mixed Rossby-gravity (Yanai) waves (e.g, small amplitudes near the equator).

Equatorial wave theory predicts that for periods between about 5-7 days and 3-4 weeks, only Kelvin and Yanai waves can propagate along the equator. The energy in these waves can only propagate eastward, hence, upon reaching the eastern boundary, all their energy must travel poleward along the coast because westward reflection is not possible in this band (Moore and Philander, 1977; Clarke, 1983). It is therefore necessary to understand the characteristics of these two equatorial wave types in order to detect their presence, determine their relative importance and

relate them to the coastal variability we find in this intermediate frequency band. Thus, for example, Yanai waves (unlike Kelvin waves) have an antisymmetric sea level structure about the equator; the only coastal indication of a Yanai origin will be an out-of-phase relationship between northern and southern hemisphere coastal tide gauges. Within the equatorial waveguide, however, Yanai and Kelvin waves have very distinctive amplitude and phase structures that can be used to discriminate between the two wave forms and determine the dominance of one type of wave over the other.

Kelvin and Yanai waves have already been detected in the equatorial waveguide for different periods. Wyrtki (1975) describes the ENSO events in terms of the generation of an equatorial Kelvin wave (eastward propagation) as the result of the relaxation of the winds in the western and central Pacific. Eriksen et al (1983) have studied sea level fluctuations in the 1-6 week period band during the 1978-1980 period at equatorial Pacific islands and have found wind-generated Kelvin waves traveling across the Pacific. Ripa and Hayes (1981) studied the meridional structure of sea level in the eastern equatorial Pacific and recognized the presence of Kelvin and Yanai waves in the first and second EOF modes of a cross-equatorial array of subsurface pressure gauges. Meridional and zonal sea level structures around the Galapagos Islands were also studied by Chiswell et al (1987) for the 1982-1983 ENSO period. They were able to identify the presence of Yanai waves at periods of 6-10 days.

Having enough evidence to support the idea that the coastal signal has an equatorial origin, we have used data from coastal and equatorial stations (Figure III.1) to extract both the Kelvin and Yanai components of equatorial variability and to compare these components to the propagating response along the coast.

For this analysis we have obtained the hourly tide heights from tide gauges (TG) in Colombia, Ecuador and Peru as well as dynamic height time series from inverted echo sounders (IES) that were deployed in a box array around the Galapagos; this is the same data used by Chiswell et al, (1987). We also have time series of subsurface pressure from pressure-temperature gauges (PTG) deployed in the Galapagos Islands. The characteristics and processing of this data set have been described by Ripa and Hayes (1981), (Figure III.1 and Table III.1). Following a discussion of the theoretical characteristics of equatorial waves (Section III.2), and description of the data (Sections III.3 and III.4), cross equatorial spectral analysis and frequency domain empirical orthogonal function (FDEOF) analysis are applied to the time series for the 1982-1983 period bracketing the latest ENSO episode (Sections III.5 and III.6). The results show that equatorially trapped Yanai waves were the principal cause of the propagating variability found in the 8-11 day band of coastal sea level by Cornejo-Rodriguez and Enfield (1987).

III.2 BACKGROUND ON EQUATORIAL WAVES

The governing equations for equatorial long waves were first developed by Laplace for shallow water on a rotating sphere. The solution to this set of equations consists of an infinite set of "meridional modes" that obey the following dispersion relation (see Gill, 1982),

$$(\omega/c)^2-k^2-\beta k/\omega=2(n+1)\beta/c \qquad \text{(III.1)}$$

where ω is the frequency, k is the wavenumber, c is a separation constant (also the gravity wave speed), f is the Coriolis parameter, n is the wave mode, $\beta=df/dy$ and y is the meridional coordinate. This relation gives us a family of curves in k,ω space that we refer to as the dispersion diagram for equatorial waves, since each curve illustrates the dispersion relation for a separate equatorial wave mode. The dispersion curves for a subset of the solutions of (III.1) are plotted in Figure III.2 as a function of dimensionless frequency (ordinate) and wavenumber (abcissa). The slope of an imaginary line connecting the origin with points (ω,k) on a curve gives the phase velocity (ω/k) of the wave with the corresponding period and wavelength. The slope of a straight line tangent to the curve at the same point gives the group velocity (rate of propagation of energy). For positive wavenumbers we have eastward phase propagation, and for negative wavenumbers, the phase propagation is towards the west. There are four classes of waves

shown: the Kelvin wave (n=-1); the inertia-gravity waves ($\beta k/\omega$ small, $n \geq 1$, high frequencies); the Rossby waves (ω^2/c^2 small, $n \geq 1$, low frequencies); and the mixed Rossby-gravity wave, or Yanai wave (n=0). The mixed Rossby-gravity (Yanai) wave derives its name from the fact that it approaches the dispersion characteristics of the Kelvin (gravity) wave at large positive wavenumbers, and that of short Rossby waves at large negative wavenumbers. Notice that phase propagates only eastward for the Kelvin wave and only westward for Rossby modes, while inertia-gravity and Yanai waves may propagate in either sense. Energy propagates only eastward for Kelvin and Yanai waves but in either sense for inertia-gravity and Rossby waves.

Note that there is a range of frequencies with upper and lower bounds at ω_u and ω_l, within which neither inertia-gravity nor Rossby waves can exist (Figure III.2). Energy in this frequency gap can only propagate eastward, in the form of Kelvin and Yanai waves. This means that if wave energy at these frequencies impinges on the eastern boundary (e.g. the coast of Ecuador in the Pacific) it is not possible for the energy to be reflected, i.e., in the form of (k<0) inertia-gravity waves or long Rossby waves (Clarke, 1983). The corresponding range of wave periods for a typical separation constant of c=2.5-3.0 m s^{-1} (first baroclinic mode) extends from 5-6 days to 30-33 days. Hence, equatorial wave variability with periods in the range of 1-4 weeks must take the form of Kelvin or Yanai waves whose energy propagates only eastward.

At the eastern boundary the incident energy must continue

poleward into either hemisphere as coastal trapped waves. Poleward of the point of incidence, the coastal wave variability will have a set of unique characteristics that do not depend on the nature of the equatorial waves from which it arises. The coastal waves are hybrid, i.e., they depend on both the topography of the continental margin and on the density structure in the water column. At sufficiently low latitudes (e.g., equatorward of 15°) they behave much like internal Kelvin waves trapped by a vertical boundary (Gill, 1982) because the offshore scale of the waves is typically larger than the scale of the coastal topography (Allen and Romea, 1980; Brink, 1982). Hence, the coastal waves along the coast of Colombia, Ecuador and north-central Peru are primarily controlled by the density stratification of the coastal ocean and are not to be confused with their high latitude counterparts, primarily controlled by topography (continental shelf-waves; see Wang and Mooers, 1976).

Since we are primarily interested in the 1-2 week period range we will describe some of the properties of the two kinds of equatorial trapped waves that occur in this band: Kelvin and Yanai waves.

Kelvin waves propagate eastward nondispersively, with water particle velocities that are everywhere parallel to the equator. The Kelvin wave has a maximum sea level displacement at the equator (Figure III.3), which falls off symmetrically to the north and south with a Gaussian shape. The decay distance is called the equatorial radius of deformation (Gill, 1982). Typical values of the

deformation radius are 100-250 km for baroclinic ocean waves with phase speeds in the range 0.5-3.0 m s^{-1}. For typical stratification found in the equatorial Pacific, phase speeds for the first baroclinic mode fall in the range 2.5-3.0 m s^{-1} and have been observed frequently at low frequencies (e.g., Knox and Halpern, 1980; Eriksen et al 1984; Lukas et al, 1984).

In Figure III.4 (upper panel) we show the Kelvin and Yanai phase spectra for two, hypothetical sea level stations located near the equator with a zonal separation of 1000 km, assuming a separation constant of 2.5 m s^{-1}. Calculated values of the phase lie between -180 and +180 degrees (the principal values of the arc tangent function) so that physical phases differing by 360 degrees are indistinguishable). Hence, the phase spectrum consists of a group of sloping lines instead of a single line extending to high phase values outside the $\pm 180^{\circ}$ domain. We refer to this phenomenom as "phase wrapping". Note that the "true" Kelvin wave phase relationship is simply a straight line extending toward positive phase, i.e., it represents physical phase that increases linearly (nondispersively) in the eastward direction at a single propagation speed (2.5 m s^{-1} in the present example).

The Yanai wave is antisymmetric about the equator (Figure III.3), with extrema near 3-4 degrees North/South and no displacement at the equator. Note that the Yanai dispersion curve (Figure III.2) crosses the frequency axis at zero wavenumber (k=0) where $\omega=\omega_0=(\beta c)^{1/2}$. For a typical value of c=2.5 m s^{-1} this occurs

at a period of 9.6 days. We call this point the "Yanai crossover" and denote the corresponding period as T_0. The crossover point is special because the phase speed (ω/k) goes through a discontinuity there, being negative to the left and positive to the right of the frequency axis. At the crossover we effectively see the superposition of two waves with infinite wavelengths and phase speeds, one traveling east, the other west (Figure III.4). This superposition yields a standing wave of infinite wavelength (the energy, however, propagates eastward).

The propagation of Yanai waves at 1-2 week periods results in a very different phase spectrum from that of a Kelvin wave. This is shown in Figure III.4 (upper panel) for two sea level stations located on the same side of the equator at an east-west separation of 1000 km. The true phase of the Yanai wave in our example crosses the zero phase axis at $T_0=2\pi\omega_0^{-1}\approx$ 9.6 days. The Yanai waves are highly dispersive, traveling westward ($T>T_0$) or eastward ($T<T_0$) depending on frequency, or not at all when they consist of standing oscillations near $T=T_0$.

III.3 DATA SETS

Our study is based primarily on sea level time series during 1982-1983, taken from tide gauges (TG), inverted echosounders (IES) and subsurface pressure-temperature gauges (PTG) located along the

coast and in the equatorial zone surrounding the Galapagos. The stations are listed in Table III.1 and shown in Figure III.1.

We use data from four coastal TGs and one near the equator in the Galapagos: Buenaventura, La Libertad, Talara-Paita, Callao and Santa Cruz. The 1982-1984 data from a tide gauge installed under the National Oceanic and Atmospheric Administration's Equatorial Pacific Ocean Climate Studies (EPOCS) program at Paita (5°S) was spliced by regression to the 1979-1981 data from Talara, (less than 50 km to the north), which subsequently deteriorated badly in quality and continuity. For the 1982-1984 period, 25 months of data are from Paita and 11 months from Talara. We refer to the combined series as Talara-Paita. To suppress the influence of the diurnal and semidiurnal tides the sea level series were low pass (LLP) filtered using a Cosine-Lanczos with a half amplitude near 40 hours and then decimated to obtain 12 hourly series. The PTGs were deployed under the EPOCS program at three island locations in the Galapagos: Wolf Island, North Isabela and South Isabela. The PTG data was kindly provided by S. Hayes (Pacific Marine Environmental Laboratory). Four inverted echo sounders were deployed in the eastern Pacific in a box array around the Galapagos as part of EPOCS. The IES gauges at 3°N,95°W, 3°N,85°W and 2°S,85°W yielded useful records and the filtered IES series were kindly provided by M. Wimbush (University of Rhode Island). A complete description of the IES instruments, their calibration and reliability is given by Chiswell et al (1987). Both the PTG and IES data have been

processed and filtered in manners analogous to our own TG data (Ripa and Hayes, 1981; Chiswell et al, 1987). For some of our analyses it was necessary to remove very long time scale variability, hence the LLP series were further smoothed, using a very low pass (VLP) filter with a half amplitude near 30 days, and the VLP series were substracted from the LLP series.

We use several different approaches to detect the presence of Kelvin and Yanai waves during the 1982-1983 ENSO event. First, a simple cross-spectral analysis is performed between Buenaventura (3°54'N) and Talara-Paita (4°37'S) sea levels, because the only coastal indication of a Yanai origin will be an out-of-phase relationship between northern and southern hemisphere stations. Second, sums and differences of band-passed cross-equatorial station pairs were calculated. Yanai waves were enhanced by differencing and supressed by summing while the opposite is true for Kelvin waves. Cross spectra between both the summed series and differenced series and the off-equatorial stations were calculated to determine the presence of Yanai and Kelvin wave energy. To identify the dominant form of equatorial variability that affects the coast we perform a frequency domain empirical orthogonal function (FDEOF) analysis based on the spectral estimates of all series in the 8-11 day period band where Cornejo-Rodriguez and Enfield (1987) found the strongest signal.

III.4 ENHANCED VARIABILITY DURING EL NIÑO EPISODES

Before proceeding further, we wish to emphasize the special character of the 1-2 week fluctuations in Peru coastal sea level found by Cornejo-Rodriguez and Enfield (1987). They showed that this variability was as much as an order of magnitude larger than before or after the intense 1982-1983 El Niño. They also pointed out that similar propagating variability has been studied by other workers for the 1976-1977 time period, which was a moderate El Niño, but that such fluctuations were apparently weaker during the intervening (non-ENSO) years. To put our 1982-1983 observations in historical perspective, we will now show that enhanced sea level variability is indeed a characteristic feature along the Peru coast during ENSO occurrences, and discuss our data set in relation to these increases.

To do this, we processed fifteen years of hourly sea level from Callao from 1970 through 1984, which includes three known ENSO episodes: 1972-1973, 1976-1977 and 1982-1983. To determine the distribution of energy with time as well as with frequency the autospectrum was computed for the LLP series for successive 250 day segments of data. The data segments are centered at 50 day intervals with a 200 day overlap between segments. The spectrum was then smoothed by applying a running band average with 10 degrees of freedom (df). The log of the spectral density is contoured and shown in Figure III.5.

The time and frequency distribution of the variance shows an increase at some frequencies during the 1972-1973 (intense) and the 1976-1977 (moderate) ENSO events, similar to but not as dramatic as in the 1982-1983 ENSO. In particular, there is a nearly tenfold increase of the variance in the 8-11 day band during 1982-1983. A similar increase of nearly the same magnitude occurred in 1972-1973 and another, less pronounced, increase in 1976-1977. In the case of the 1982-1983 data, Cornejo-Rodriguez and Enfield (1987) found that the most energetic signals (in the 8-11 day) band were propagating poleward along the eastern boundary as unforced coastal trapped waves.

Figures III.6 shows that the high frequency variability in the band passed (LLP-VLP) series is not stationary in time. There is an increase in the rms amplitudes of these series during the 1982-1983 ENSO episode visually apparent at some of the stations. This increase is not statistically significant at the PTG stations, Wolf Island, North Isabela and South Isabela. The small amplitude of the increase is characteristic of the equatorial stations, and as pointed out by Cornejo-Rodriguez and Enfield (1987), is consistent with the antisymmetric structure of Yanai waves.

III.5 CROSS SPECTRAL ANALYSIS

To test for coastal SLH signals that are antisymmetric about

the equator, a simple cross spectral analysis was performed between the Buenaventura and the Talara-Paita sea level series for a period including the 1982-1983 ENSO event (from September 1982 to September 1983). To smooth the cross spectrum we applied a running band average on eight successive frequencies, with five overlapping frequencies, obtaining 16 df per band and a bandwidth of 0.0204 cpd (Figure III.7).

In general, the coherence (γ) is frequently high and significant in bands centered at frequencies less than 0.20 cpd (Figure III.7, lower panel). We find 99% significant γ^2 peaks centered at 0.027, 0.073, 0.111, 0.149 and 0.180 cpd that correspond to periods of 37.0, 13.7, 9.1, 6.7 and 5.6 days. In the 8-11 day band nearly all γ^2 values are significant at the 90% confidence level. For frequencies greater than 0.20 cpd, γ^2 is generally low and seldom significant above the 90% confidence level. For the 0.0204-0.080 cpd frequency range (periods greater than 12.5 days), the phase oscillates around zero, suggesting the presence of Kelvin wave variability. For the 0.096-0.149 cpd frequency range (periods of 6.7 to 10.4 days), the phases are distributed near $\pm 180^\circ$ or are large and positive, suggesting an antisymmetric relation (Yanai signal). It is significant that Chiswell et al (1987) also find a clear antisymmetric behavior in the dynamic height data from the EPOCS IES array in this same range of frequencies. We also computed the cross spectra between Buenaventura and Talara-Paita SLH series for periods before (June 1981-June 1982) and after (December

1983-May 1984) the 1982-1983 ENSO event. We do not find similar evidence in either the coherences or the phases for Kelvin and Yanai waves. In summary, the cross-equatorial phase relationships along the coast are consistent with the dominance of Kelvin waves at periods longer than 12.5 days, and of Yanai waves at periods of 6-11 days, but only during the 1982-1983 ENSO episode.

Based on the orthogonality of the Yanai and Kelvin components we performed a cross spectral analysis between near equatorial stations. To enhance the Yanai waves and supress the Kelvin signal, we normalized the variance and differenced the band-passed series at the cross-equatorial station pairs near 92°W (SI/WI) and 85°W (2S/3N), subtracting southern series from the northern ones. The cross spectra were then computed between the differenced series and off-equatorial stations to the west and to the east (IES at 3°N,95°W; TGs at STZ, SI, LLB). The cross spectra involving the SI/WI series were computed from January 24 to July 20, 1983 and those involving 2S/3N from April 21 to October 21, 1983. Both periods are 180 days long and occur within the time frame of the 1982-1983 ENSO event when the propagating coastal variability was strong (Figures III.5 and III.6). The cross spectra were smoothed in the same way as the one between Buenaventura and Talara-Paita (Figure III.7), obtaining band averaged cross spectral estimates with 16 df.

The cross spectra involving the differenced series are shown in Figure III.8 (left panels). The coherence (Y) consistently has a

relative maximum centered near the 10-day period, a minimum at seven days and a secondary maximum near 5-6 days. Except for SI vs 2S/3N, all γ^2 values are significant at the 90% confidence level at these two peaks. Note that the 10-day peaks are smallest for pairs involving STZ and SI, which are closer to the equator than other stations. This is consistent with the dominance of Yanai wave energy, which is smallest close to the equator.

The phase estimates were normalized for the zonal separation between stations by referring them to a common zonal distance of 1000 km. The Yanai phase line (Figure III.4, upper panel) was then fitted to the independent phase estimates for coherences at 80% confidence level or greater. The fitted curve yielded an estimate of the separation constant (gravity wave speed) of 2.0-4.5 ms^{-1} and a Yanai "crossover" of T_0=7.2-10.6 days (95% confidence interval). The cluster of phases near 0° in the 8-11 day band is due to the dominant coherence there. Note also that even at low frequencies the phases adhere closely to the Yanai phase line. Given the steepness of the theoretical curve and the random variability in the phases, this agreement may be coincidental. At high frequencies (periods shorter than seven days) the phases are distributed in a highly regular, linear fashion, also suggesting propagation. However, they fall mostly above the Yanai curve, suggesting slower propagation than is consistent with the lower frequencies, or that a wave type other than the Yanai may be involved.

Other cross spectra (not shown) were computed between the 2S/3N

difference series and Talara-Paita and Buenaventura series, as well as zonal cross spectra (IESs at 3°N,95°W and 3°N,85°W vs BVA; 2°S,85°W vs TPA). These cross spectra also show very high coherence in the 8-11 day band. The phase spectra are almost, but not perfectly consistent with the suggestion from Figures III.7 and III.8, i.e., that an antisymmetric response occurs at the coast in response to standing Yanai waves whose energy is incident on the eastern boundary. Zonal comparisons north or south of the equator show 8-11 day phases that are slightly skewed away from zero (east lags west). We also performed the comparison between Talara-Paita and Buenaventura for different time intervals within the ENSO time frame. The phases fall in the range between +90° and +180°, i.e., not as consistently near 180° as Figure III.7 suggests. These somewhat "imperfect" phase relationships are all consistent with the assumption that coastal propagation as coastal trapped waves begins equatorward of 4-5 degrees of latitude, and with a longer propagation time (path length) north of the equator than south of the equator (in agreement with the sharply different coastline geometries).

The cross spectra for the cross-equatorial sums are shown in Figure III.8 (right panels). The coherences are smaller than the ones found for the difference series. Again we normalized the phases by the zonal separation and referred them to a common zonal distance (1000 km). The Kelvin phase line (Figure III.4, upper panel) was fitted to phases corresponding to 80% significant

coherences, yielding an estimated gravity wave speed of c=1.9-3.3 ms^{-1}. Notice that the symmetric (Kelvin) component is complementary to the antisymmetric (Yanai) component, i.e., it tends to dominate in frequency ranges where the other is weak.

III.6 FREQUENCY DOMAIN EOF ANALYSIS

To test for the two fundamentally different wave structures on the equator and their relative contributions to the coastal variability, we subjected the entire suite of sea level and pressure observations to a frequency domain EOF (FDEOF) analysis in the 8-11 day band where the coastal signal was strongest (see Cornejo-Rodriguez and Enfield, 1987). Because the Kelvin and Yanai modes are orthogonal, they separate into distinct FDEOF components with characteristic amplitude and phase structures.

The FDEOF analysis was performed on a common data period extending from mid-April to end of July, 1983, comprising about 11 realizations of a process having a 9-10 day periodicity. The first FDEOF component, which extracts the dominant variability , explains 69% of the overall variance in the 8-11 day band. The second FDEOF mode explains 14% of the variance. By the EOF mode selection rule of Overland and Preisendorfer (1982) we find that only the first FDEOF component is significant at the 95% confidence level. The statistics listed in Table III.2 show that large fractions (64-91%)

of the 8-11 day variance in the coastal SLH variability are associated with the first mode. The phases are antisymmetric about the equator and amplitudes increase away from the equator toward higher latitudes, as expected for Yanai waves. In contrast, the amplitude and phase structures of the second FDEOF mode do not exhibit characteristic, interpretable patterns (such as one might expect for Kelvin waves, for example).

The contoured distributions of the first FDEOF mode phase and amplitude are shown in Figure III.9 and were constructed in the following manner. The first mode phases and amplitudes listed in Table III.2 were assigned to the corresponding station locations, shown as solid circles in Figure III.9. However, in order to produce coastal contours at latitudes greater than $\pm 3^{\circ}$ where oceanic data were absent, it was necessary to introduce artificial values of amplitude and phase at points offshore (in a perpendicular sense) of the tide stations at Buenaventura, Talara-Paita and Callao (crosses). The phase assigned to each of the offshore points was just equal to the phase at the corresponding coastal point, consistent with poleward phase propagation at the coast. Amplitudes at the offshore points were decreased from the corresponding coastal values by an amount consistent with free coastal trapped waves in which the Rossby radius of deformation is the relevant offshore decay scale. Finally, for added clarity, all amplitudes south of the equator were assigned negative values in agreement with the negative sign of the corresponding phases. Because of the

artificial points introduced, we attribute no significance to the contoured indications of amplitude decay and phase invariance offshore of the coastal tide stations, except to say that the FDEOF results are consistent with a simple trapped wave interpretation.

The phases for the first mode are clearly antisymmetric, changing sign from +90° at stations north of the equator to -90° south of the equator (Figure III.9). This is consistent with the antisymmetric character of Yanai waves (Figure III.3). Because the contouring program interpolates between stations, it appears that phase changes smoothly across the equator. In fact, it is discontinuous, as it should be (Table III.2). This can be seen as a "pinching" of the contoured phase lines where stations are found closer to the equator (in the Galapagos). The generally zonal orientation of phase lines in the equatorial zone is consistent with a standing oscillation, as expected near the Yanai crossover ($T_0 \approx 10$ days). Southward along the Peru coast, phase advances to negative values of larger magnitude, consistent with the conversion of the Yanai waves into poleward propagating, coastal trapped Kelvin waves. The rms amplitudes are small near the equator and largest at the higher latitude coastal stations. This is also consistent with the antisymmetric meridional displacement profile of Yanai waves.

In summary, the dominant mode of 8-11 day variability in the eastern equatorial Pacific has antisymmetric displacement structure consistent with stationary, Yanai waves, and these are clearly related to most of the Peru coastal variability during the 1982-1983

ENSO episode. We can find no concrete evidence for the existence of Kelvin waves in this frequency band and the remaining (unexplained, higher mode) variability probably consists mostly of unstructured noise.

III.7 SUMMARY AND DISCUSSION

The lack of simultaneous measurements at coastal, equatorial and off-equatorial oceanic stations has prevented previous studies from establishing a convincing connection between equatorial variability and energetic coastal signals during previous ENSO events (e.g., Romea and Smith, 1983). Now, however, the combined coastal and equatorial data available to us from the 1982-1983 time frame provide strong evidence that the enhanced 1-2 week propagating variability off Peru-Ecuador during the El Niño originated in the equatorial waveguide, primarily as mixed Rossby-gravity (Yanai) waves.

The tendency for the Yanai waves to dominate in the 8-11 day band and Kelvin waves at lower frequencies appears repeatedly in our analysis and is consistent with the observations of others (e.g., Lukas et al 1984, Chiswell et al 1987). The coastal cross spectrum between Buenaventura and Talara-Paita suggests the presence of Kelvin waves for frequencies smaller than 0.08 cpd (periods greater than 13 days) and the presence of Yanai waves for periods of 7-10

days, approximately where the coastal signal was most energetic during the 1982-1983 ENSO (Figure III.5, see also Cornejo-Rodriguez and Enfield, 1987). The analysis of simultaneous SLH records of coastal, equatorial and off-equatorial stations in the eastern equatorial Pacific has shown the dominance of the Yanai signal over the Kelvin waves in the 8-11 day band, where the coherence was much higher for antisymmetric than for symmetric variability (Figures III.8, III.9). The antisymmetric phase spectrum (Figure III.8) was consistent with a Yanai crossover at T_0=7.2-10.6 days and both the symmetric and antisymmetric spectra were consistent with gravity wave speeds of 2.0-4.5 m s^{-1} along the equator. Finally, the FDEOF analysis (Table III.2, Figure III.9) shows clearly that most of the 8-11 day energy along the coast is associated with meridionally antisymmetric displacement variability along the equator and zonally invariant phase, consistent with the existence of standing Yanai oscillations at frequencies near the Yanai crossover.

It has often been observed (e.g., Wunsch and Gill, 1976) that certain energetic frequencies tend to recur in near-equatorial ocean spectra. The Yanai dominance in the 8-11 day band is another example of this. The most probable reason for the band-specific behavior is that the dominant meteorological forcing scales in the equatorial Pacific are large over a wide range of frequencies (Luther, 1980). The large-scale forcing excites low wavenumber ocean waves most easily (McCreary, 1984). As can be seen in the dispersion diagram for equatorial waves (Figure III.2), this occurs

for Kelvin and long Rossby waves at the lowest frequencies (e.g., Eriksen et al 1983; Lukas et al 1984; Ripa and Hayes 1981), for locally resonant inertia-gravity waves at high frequencies (Wunsch and Gill 1976; Luther, 1980; Chiswell et al, 1987), and for Yanai waves in the 1-2 week period range, near the Yanai crossover.

Two hypotheses may be formulated about how the equatorial Yanai signals are generated. One is that they are generated by zonal and/or meridional wind fluctuations in the equatorial Pacific, west of the Galapagos. The other is that they are excited internally within the ocean, possibly by instability waves within the equatorial waveguide (Philander, 1976,1978; Cox, 1980). A search for the ultimate source of these waves is beyond the scope of this paper, but may be addressable through a combination of modeling and further data analysis. One of the most interesting tasks of such an analysis will be to explain why Yanai variability is preferentialbly forced and/or transmitted to the eastern boundary during El Niño episodes.

Table III.1-Given for each station is its name, abbreviation, location and data source. Data sources are: University of Hawaii (UH), Instituto Oceanografico de la Armada del Ecuador (INOCAR), Direccion de Hidrografia y Navegacion de la Marina del Peru (DHNM), Corporacion de Aviacion Civil del Peru (CORPAC), the Instituto Geografico Agustin Codazzi de Colombia (IGAC), the National Oceanic and Atmospheric Administration's Equatorial Pacific Climate Studies (EPOCS) program, University of Rhode Island (URI) and Pacific Marine Environmental Laboratory (PMEL). The Talara and Paita sea level series have been combined (see text) and referred to as Talara-Paita (TPA).

Sea Level Station	Abbr	Lat.	Lon.	Source
Buenaventura	BVA	3°54'N	77°05'W	IGAC
La Libertad	LLB	2°12'S	80°55'W	INOCAR
Santa Cruz	STZ	0°45'S	90°18'W	UH
Talara	TPA	4°37'S	81°17'W	DHNM
Paita		5°05'S	81°07'W	EPOCS
Callao	CAL	12°03'S	77°09'W	DHNM
Wolf Island	WI	1°24'N	91°50'W	PMEL
North Isabela	NI	0°03'S	91°28'W	PMEL
South Isabela	SI	0°59'S	91°30'W	PMEL
Echosounder	IES	3°00'N	95°00'W	URI
Echosounder	IES	3°00'N	85°00'W	URI
Echosounder	IES	2°00'S	85°00'W	URI

Table III.2- Characteristics of the first FDEOF mode. The arbitrarily referenced phases computed by the FDEOF program were adjusted by adding a constant value to all phases so as to obtain a value of +90° at 3°N,85°W. Station abbreviations are listed in Table III.1

Sea Level Station	Band variance (cm^2)	Rms amplitudes (cm)	Expl. variance (%)	Phase (°)
3°N 95°W	2.38	1.081	49	+69
3°N 85°W	0.60	0.665	74	+90
2°S 85°W	1.29	0.874	59	-91
WI	2.91	0.962	32	+90
NI	1.16	0.333	10	-63
SI	1.29	0.427	14	-86
STZ	1.68	0.892	47	-100
BVA	6.42	2.027	64	+7
LLB	9.62	2.874	86	-78
TPA	8.82	2.830	91	-118
CAL	4.93	1.856	70	-248

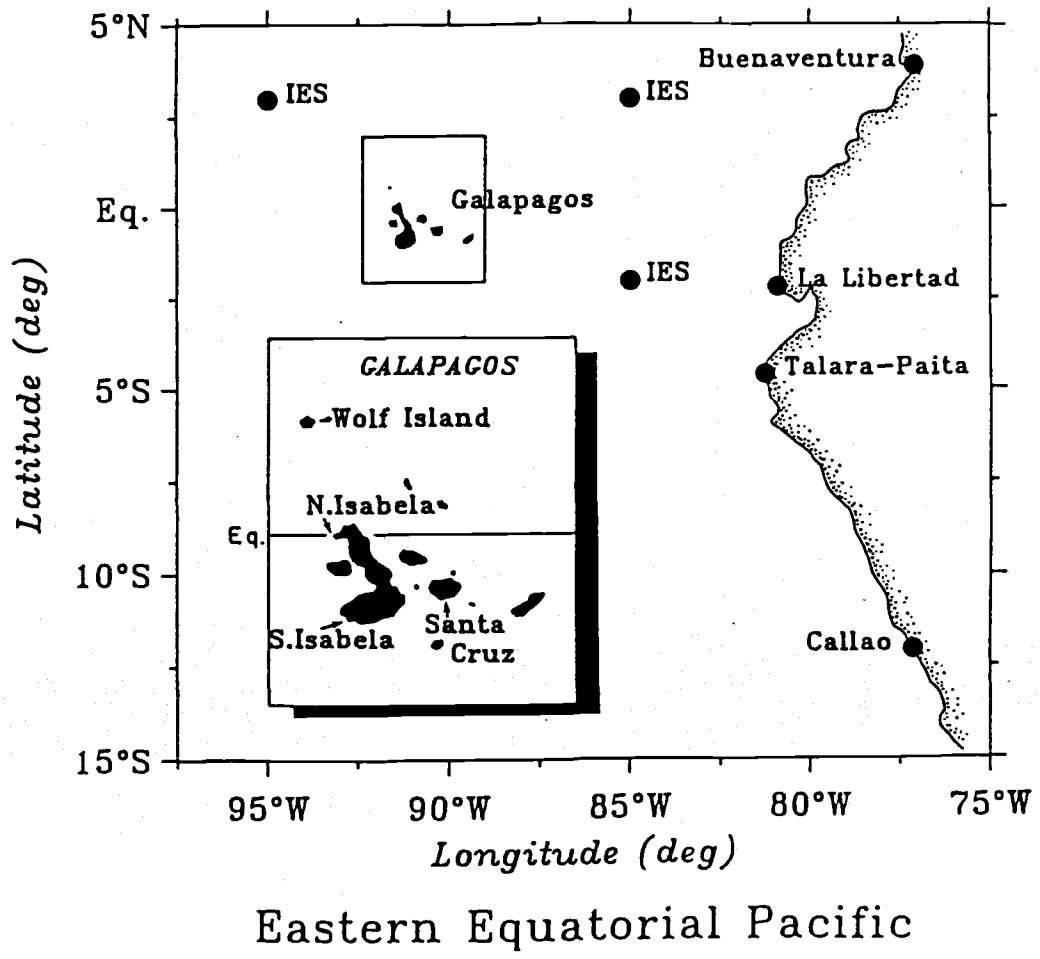

Figure III.1 Background: locations of coastal tide gauge stations and oceanic inverted echo sounder stations. Foreground (inset): location of Santa Cruz tide gauge and the three pressure-temperature gauges within the Galapagos Archipelago.

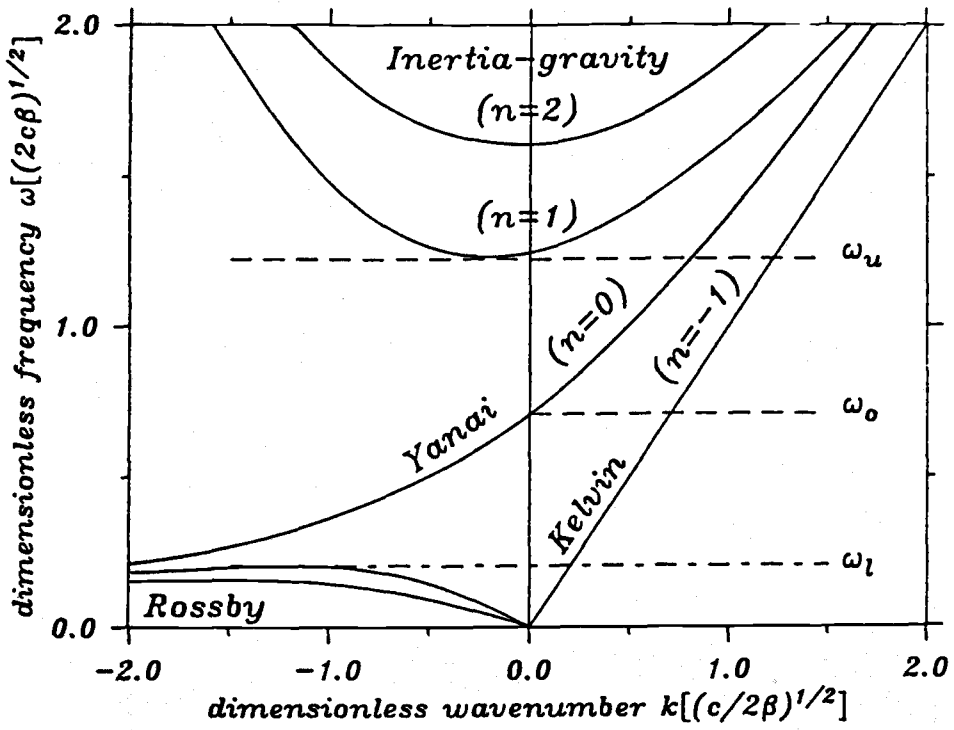

Dispersion Diagram of Equatorial Waves

Figure III.2 Theoretical dispersion relation for equatorial waves. The vertical axis is the nondimensional frequency (ω) scaled by $(2\beta c)^{1/2}$ and the horizontal axis is the nondimensional wavenumber (k) scaled by $(2\beta/c)^{1/2}$, where c=2.5 m s^{-1}. The reflectionless gap is defined by the upper and lower bounds ω_U=1.22 and ω_1=0.20. The Yanai crossover occurs at ω_o=0.70 (see the discussion in the text).

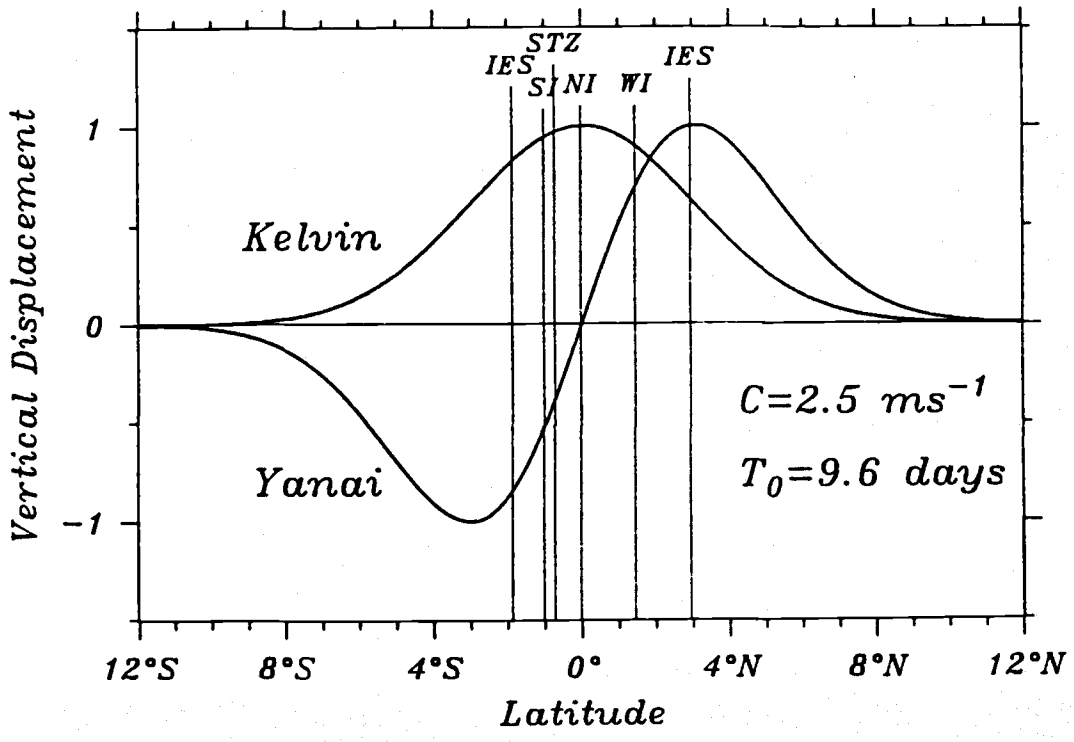

Meridional Profiles of Equatorial Waves

Figure III.3 Meridional surface displacement profiles for equatorial Kelvin and Yanai waves. The sea level displacement is computed for a separation constant c=2.5 m s^{-1}. The vertical lines indicate the meridional locations of stations shown in Figure III.1 and discussed in the text, and whose abbreviations are defined in Table III.1.

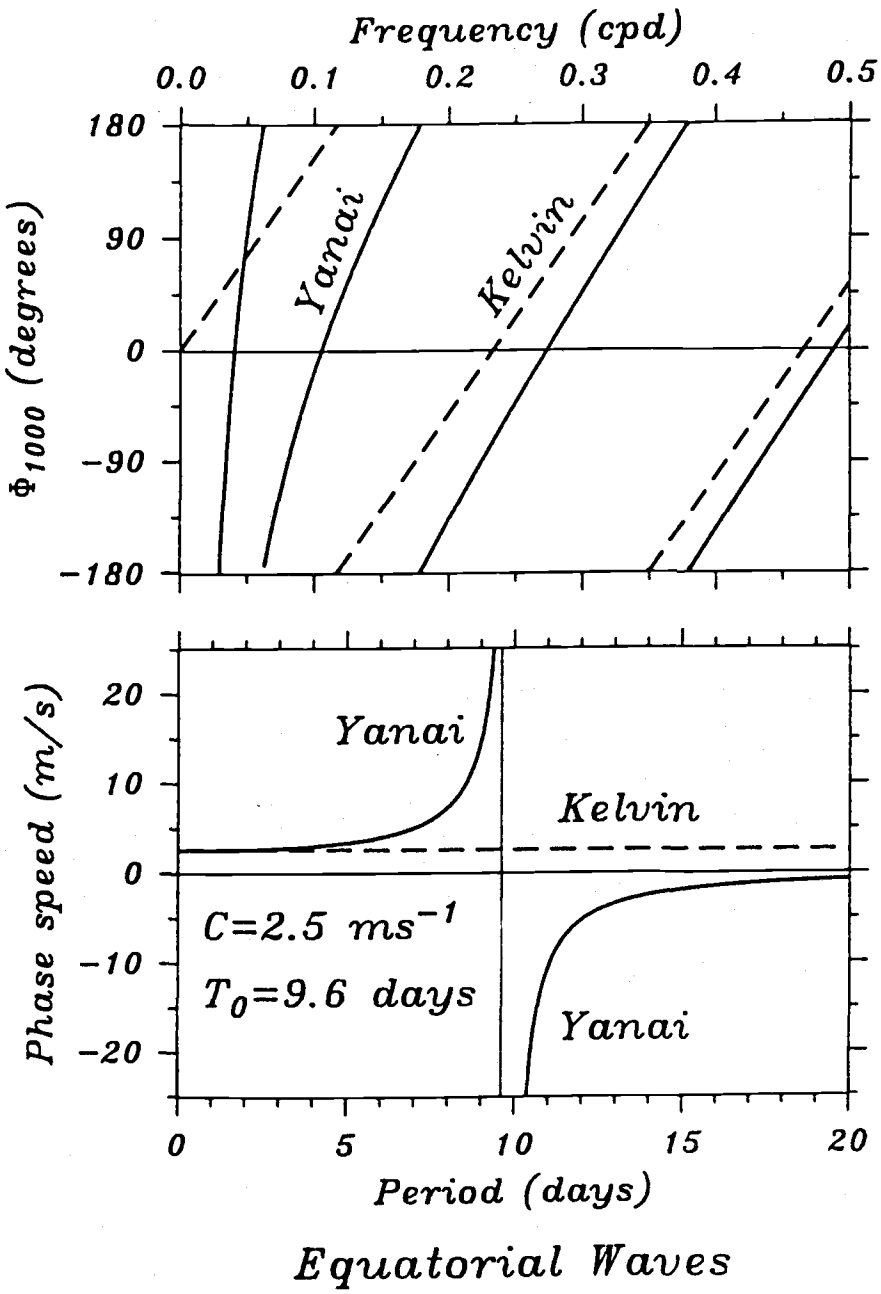

Figure III.4 Upper panel: phase spectra for Yanai and Kelvin waves for two sea level stations located near the equator with a zonal separation of 1000 km. Phase advances toward positive values for eastward propagation. Note that for periods near the Yanai crossover (T_0), waves are nearly in phase due to their very large phase speeds. Kelvin waves at similar periodicities are nearly 180° out of phase. Lower panel: phase speed as a function of the period. In both panels, solid and dashed curves refer to Yanai and Kelvin waves, respectively.

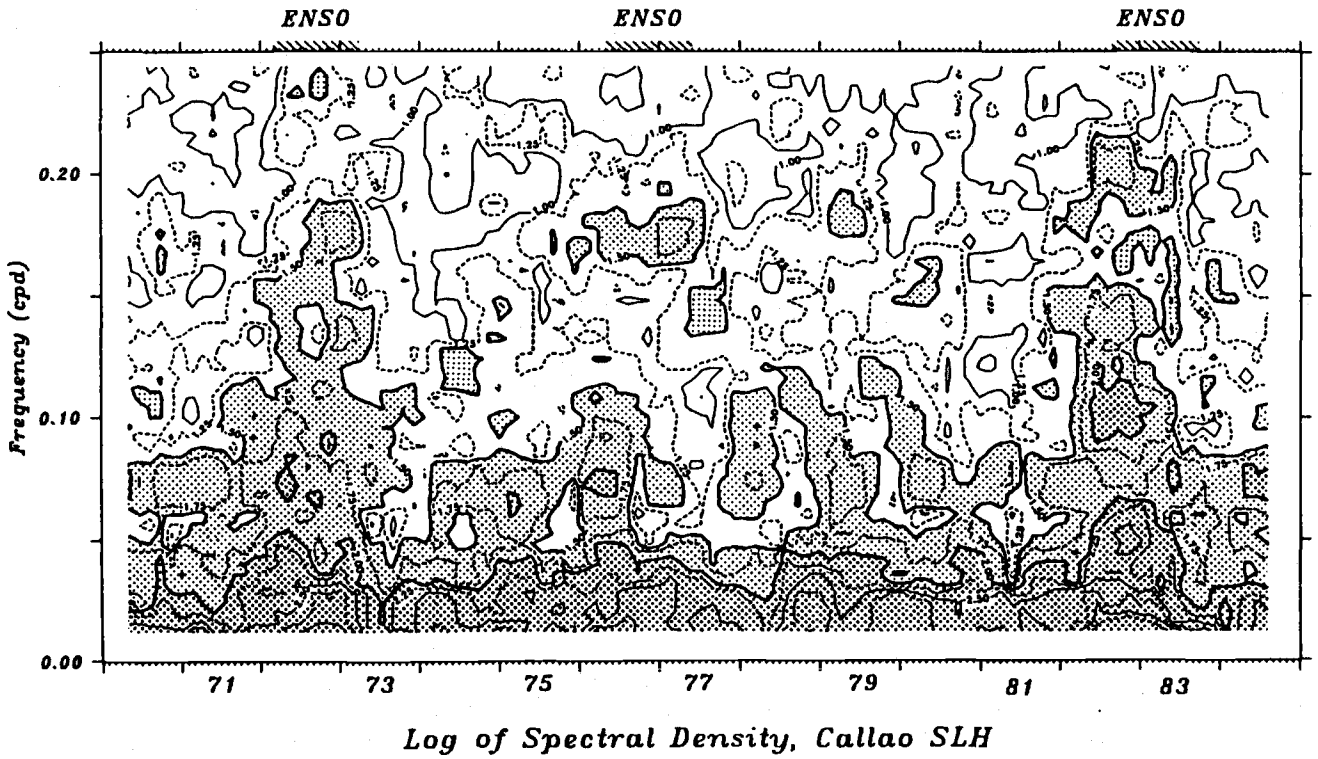

Figure III.5 Contour plot of the log of spectral density (cm^2 day) as a function of time and frequency for the sea level at Callao. The chance probability that a feature lies more than 0.26 above a given value is less than 10%. Dark (light) shading indicates log values above 2.0 (1.5).

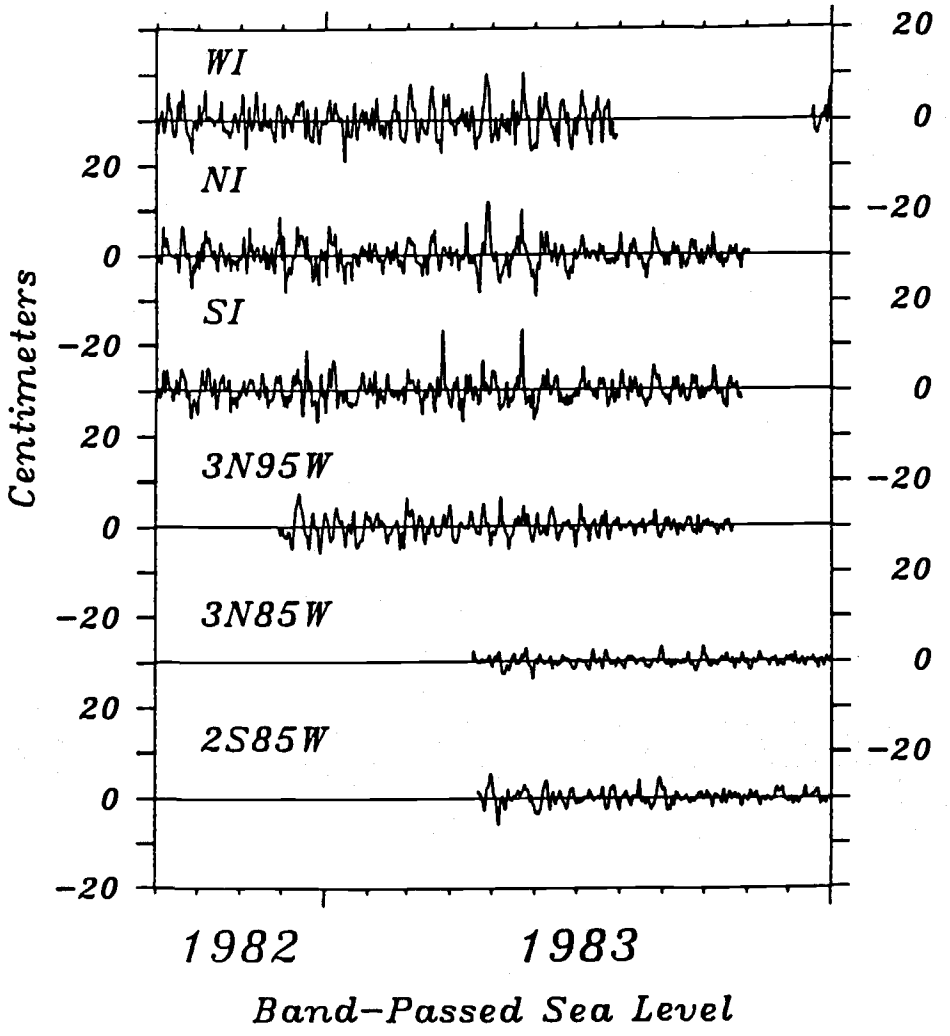

Figure III.6 Band-passed (2-30 days) time series of sea level at equatorial stations shown in Figure III.1. The means have been removed.

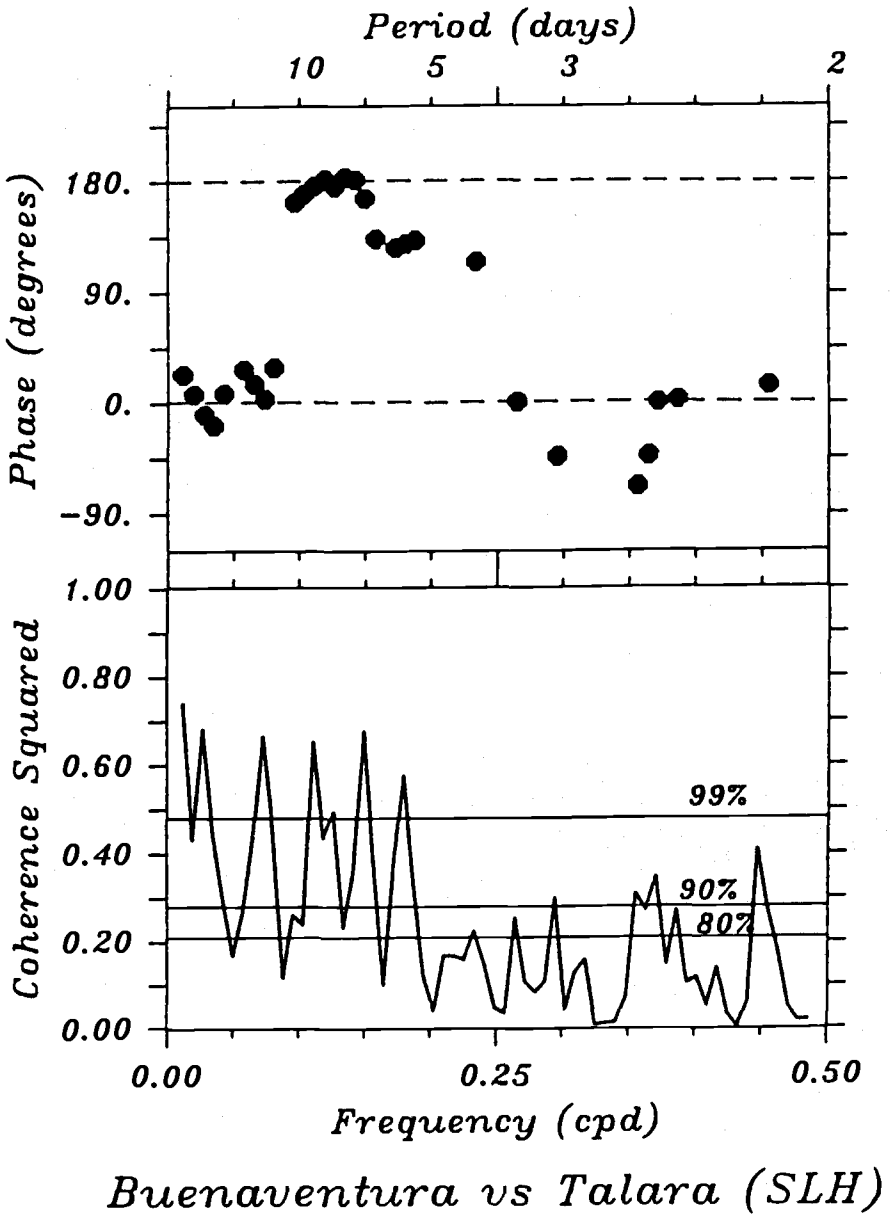

Figure III.7 Cross spectrum between Buenaventura and Talara-Paita. Upper panel: phase estimates plotted for γ^2 values at the 80% confidence level or higher. Buenaventura leads Talara-Paita for positive lags. Lower panel: coherence spectrum with the γ^2 significance levels shown for various degrees of statistical confidence.

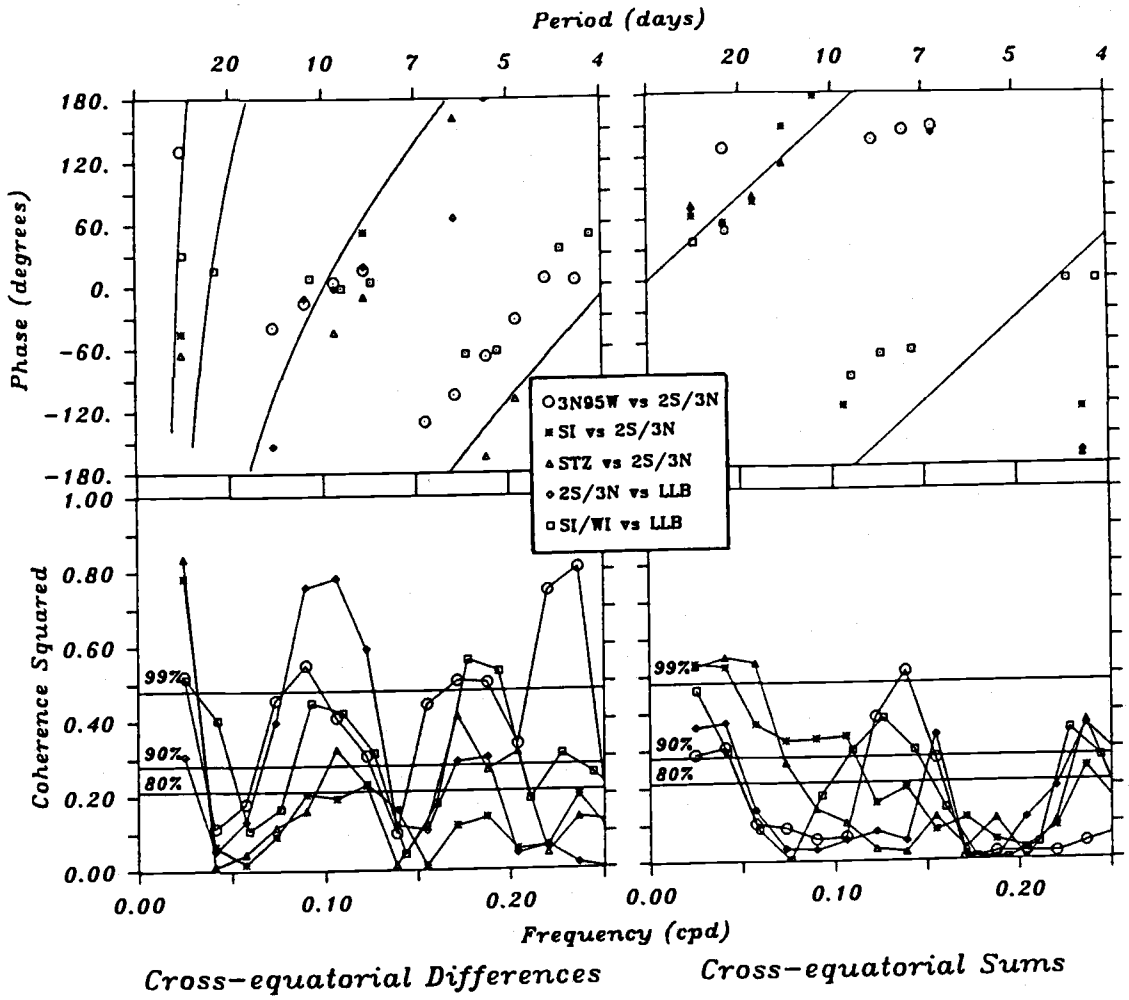

Figure III.8 Left panels: phase and coherence spectra for cross-equatorial difference series versus data at stations to the east or west. Right panels: phase and coherence spectra for cross-equatorial sum series versus data at stations to the east or west. Station abbreviations used in the legend are defined in Table III.1. The curved and straight phase lines correspond to the theoretical phase spectra for Yanai and Kelvin waves, respectively, fitted to the observed phases by least squares.

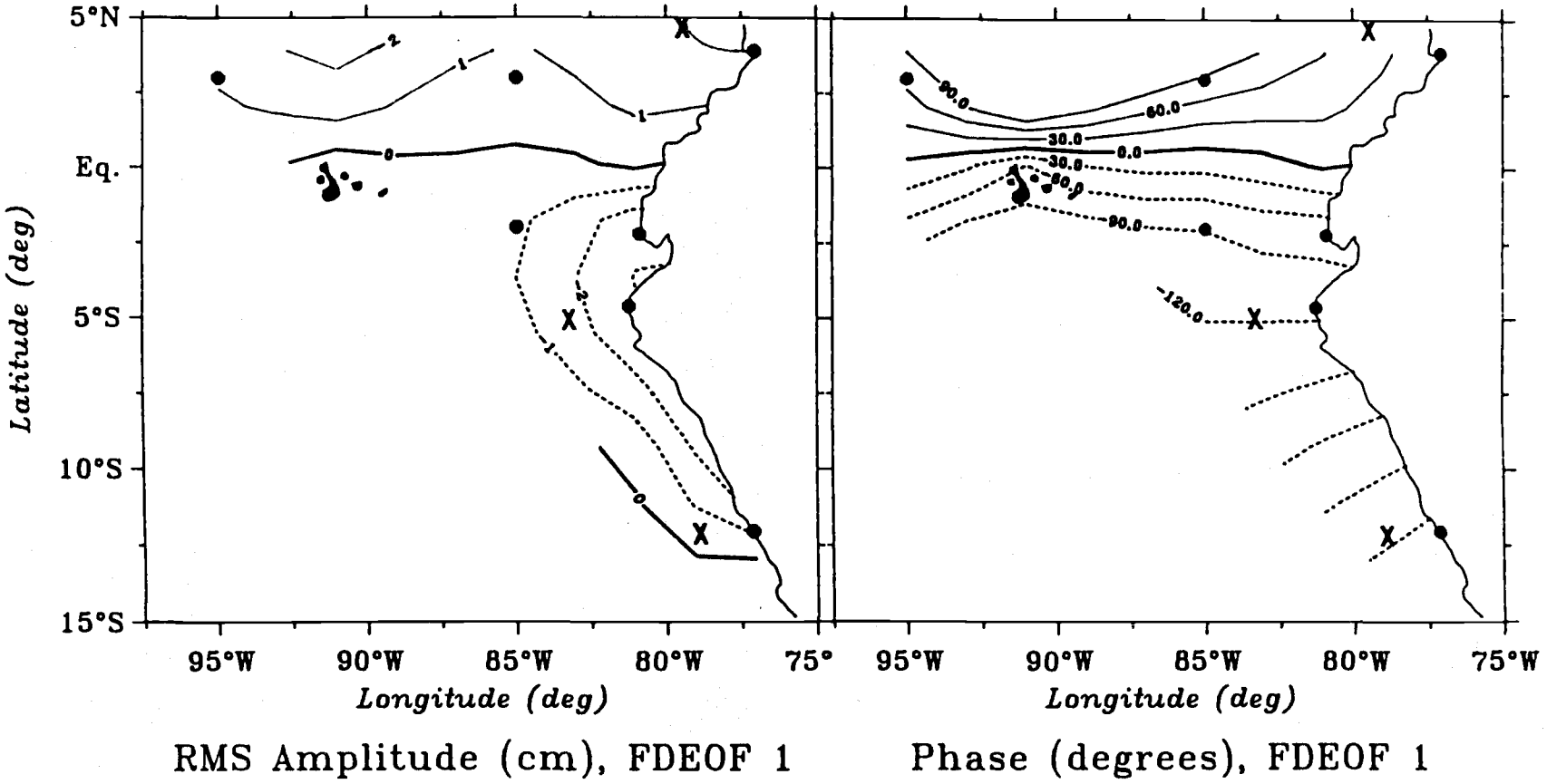

Figure III.9 Left panel: rms amplitudes of the first FDEOF mode in the 8-11 day band. Right panel: the corresponding phases. Amplitudes have been assigned the same signs as the phases for added clarity.

REFERENCES

Chiswell, S.M., D.R. Watts and M. Wimbush, Inverted echo sounder observations of zonal and meridional dynamic height variability in the eastern equatorial Pacific during the 1982-83 El Niño. Deep Sea Res., in press, 1987.

Clarke, A.J., The reflection of equatorial waves from oceanic boundaries, J. Phys. Oceanogr., 13, 1193-1207, 1983.

Cornejo-Rodriguez, M.P. and D.B. Enfield, Propagation and forcing of high frequency sea level variability along the west coast of South America, submitted to J. Phys. Oceanogr., 1987.

Cox, M.D., Generation and propagation of 30-day waves in a numerical model of the Pacific, J. Phys. Oceanogr., 10, 1168-1186, 1980.

Eriksen, C.C., M.B. Blumenthal, S.P. Hayes and P. Ripa, Wind-generated equatorial Kelvin waves observed across the Pacific ocean, J. Phys. oceanogr., 13, 1622-1640, 1983.

Gill, A.E., Atmosphere-ocean dynamics, Academic Press Inc., New York, 1982, 662 pp.

Knox, R. A. and D. Halpern, Long range Kelvin wave propagation of transport variations in Pacific ocean equatorial currents, J. Mar. Res., 40, 329-339, 1982.

Lukas, R., S.P. Hayes and K. Wyrtki, Equatorial sea level response during the 1982-83 El Niño, J. Geophys. Res., 89, 10,425-10,430, 1984

Luther, D.S., Observations of long period waves in the tropical oceans and atmosphere, Ph. D. Thesis, Massachusetts Institute of Technology, Woods Hole Oceanographic Institution, February 1980, 210 pp.

Mc Creary, J.P., Equatorial beams, J. Mar. Res., 42, 395-430, 1984.

Moore, D.W. and S.G.H. Philander, Modelling of the tropical ocean circulation, The Sea, Ch. 8, Vol. 6, Goldberg et al Eds., Interscience, New York, 1977.

Overland, J.E. and R.W. Preisendorfer, A significance test for

principal components applied to a cyclone climatology, Month.Wea. Rev., 110, 1-4, 1982.

Philander, S.G.H., Instabilities of zonal equatorial currents, J.Geophys. Res., 81, 3725-3735, 1976.

---------, Instabilities of zonal equatorial currents, 2, J. Geophys.Res., 83, 3679-3682, 1978.

Ripa, P. and S.P. Hayes, Evidence for equatorial trapped waves at the Galapagos Islands, J. Geophys. Res., 86, 6509-6516, 1981.

Romea, R.D. and R.L. Smith, Further evidence for coastal trapped waves along the Peru coast. J. Phys. Oceanogr., 13, 1341-1356, 1983.

Wang, D.P. and C.N.K. Mooers, Long coastal trapped waves off the west coast of the United States, summer 1973, J. Phys. Oceanogr., 6, 856-864, 1976.

Wunsch, C. and A.E. Gill, Observations of equatorially trapped waves in Pacific sea level variations, Deep-Sea Res., 23, 371-390, 1976.

Wyrtki, K., El Niño-the dynamic response of equatorial Pacific ocean to atmospheric forcing. J. Phys. Oceanogr., 5, 572-584, 1975.

CHAPTER IV

SUMMARY

We have studied the characteristics of high (5-7 days to 3-4 weeks) frequency sea level and wind variability along the west coast of South America, establishing comparisons between Austral summer and winter seasons and also interannual comparisons between ENSO and non-ENSO years. We have used additional equatorial and off-equatorial SLH data to extract both Kelvin and Yanai components of equatorial variability and to compare these components to the propagating response along the coast, both south and north of the equator. The principal results of this study can be summarized as follows:

1. There are no significant differences in the energy levels of winds and sea level between Austral summers and winters

2. There is weak evidence for local forcing at all stations. This is responsible for only small percentages of the SLH variance, although it occurs for both seasons and for both ENSO and non-ENSO periods.

3. There is poleward propagation of SLH coastal fluctuations during the winter seasons at speeds of 2.8 m s^{-1} between Talara-Paita and Callao, consistent with previous evidence of low

mode coastal trapped waves along the Peru coast.

4. Coastal sea level was more energetic during El Niño occurrences in the 1970-1984 period (1972-1973, 1976-1977 and 1982-1983) than during non-ENSO periods.

5. The autospectra for multi-year SLH series (1979-1984) shows a tenfold increase of the variance in the 8-11 day band during the 1982-1983 ENSO event at all coastal stations. The signal is unforced along the coast and is characterized by strong alongshore coherence and a poleward phase speed of 3.5 m s^{-1}. The phase speed increase over that of non-ENSO winters is consistent with anomalous depression of the coastal density structure during the 1982-1983 ENSO.

6. The 8-11 day signal in sea level on the south side of the equator were out of phase with those north of the equator. Phase was zonally uniform along the equator indicating that the Yanai waves were standing (stationary) oscillations, consistent with theory.

7. Equatorially trapped Yanai waves were the principal source of the 1-2 week propagating variability found in the sea level records from the Ecuador-Peru coast during the 1982-1983 El Niño.

BIBLIOGRAPHY

Allen,J.S. and R.D.Romea, On coastal trapped waves at low latitudes in a stratified ocean, J.Fluid Mech., 98, 555-585, 1980.

Bigg,G.R. and A.E.Gill, The annual cycle of sea level in the eastern tropical Pacific, J.Phys.Oceanogr., 16, 1055-1061, 1986.

Brink,K.H., A comparison of long coastal trapped wave theory with observations off Peru, J.Phys.Oceanogr., 12, 897-913, 1982.

-------, J.S.Allen and R.L.Smith, A study of low frequency fluctuations near the Peru coast, J.Phys.Oceanogr., 8, 1025-1041, 1978.

Chelton,D.B. and R.E.Davis, Monthly mean sea level variability along the west coast of North America, J.Phys.Oceanogr., 12, 757-784, 1982.

Chiswell,S.M., D.R.Watts and M.Wimbush, Inverted echo sounder observations of zonal and meridional dynamic height variability in the eastern equatorial Pacific during the 1982-83 El Niño. Deep-Sea Res., in press, 1987.

Clarke,A.J., The reflection of equatorial waves from oceanic boundaries, J.Phys.Oceanogr., 13, 1193-1207, 1983.

Cornejo-Rodriguez,M.P. and D.B.Enfield, Propagation and forcing of high frequency sea level variability along the west coast of South America, submitted to J.Phys.Oceanogr., 1987.

Cox,M.D., Generation and propagation of 30-day waves in a numerical model of the Pacific, J.Phys.Oceanogr., 10, 1168-1186, 1980.

Enfield,D.B. and J.S.Allen, On the structure and dynamics of monthly mean sea level anomalies along the Pacific coast of North and South America, J.Phys.Oceanogr., 10, 557-578, 1980.

-------, Thermally driven wind variability in the planetary boundary layer above Lima, Peru, J.Geophys.Res., 86, 2005-2016, 1981a.

-------, Annual and non-seasonal variability of monthly low-level wind fields over the southeastern tropical Pacific, Mon.Wea. Rev., 109, 2177-2190, 1981b.

-------,and -------, The generation and propagation of sea level variability along the Pacific coast of Mexico, J.Phys.Oceanogr., 13, 1012-1033, 1983.

-------, M.P.Cornejo-Rodriguez, R.L.Smith and P.M.Newberger, The equatorial propagating variability along the Peru coastduring the 1982-83 El Niño, submitted to J.Geophys.Res., 1987.

-------, and P.M.Newberger, Peru coastal winds in 1982-83, Proceedings of the Ninth Annual Climate Diagnostic Workshop, Oregon State University, 22-26 October 1984. U.S. Dept. of Commerce, National Oceanic and Atmospheric Administration, pp. 147-156, 1984.

-------, The intraseasonal oscillation in eastern Pacific sea levels: how is it forced?, J.Phys.Oceanogr., in press, 1987.

Eriksen,C.C., M.B.Blumenthal, S.P.Hayes and P.Ripa, Wind-generated equatorial Kelvin waves observed across the Pacific ocean, J.Phys.Oceanogr., 13, 1622-1640, 1983.

Gill,A.E., Atmosphere-Ocean Dynamics, Academic Press Inc., New York, 1982, 662 pp.

Halliwell,G.R. and J.S.Allen, Large scale sea level response to atmospheric forcing along the west coast of North America, J.Phys.Oceanogr., 14, 864-886, 1984.

Hayes,S.P. and D.Halpern, Correlation of current and sea level in the eastern equatorial Pacific, J.Phys.Oceanogr., 14, 811-824, 1984.

Knox,R.A. and D.Halpern, Long range Kelvin wave propagation of transport variations in Pacific ocean equatorial currents, J.Mar.Res., 40, 329-339, 1982.

Leetmaa,A., D.W.Behringer, A.Huyer, R.L.Smith and J.Toole, Hydrographic conditions in the eastern Pacific before, during and after the 1982/83 El Niño, submitted to Prog. Oceanogr., 1987.

Lukas,R., S.P.Hayes and K.Wyrtki, Equatorial sea level response during the 1982-83 El Niño, J.Geophys.Res., 89, 10425-10430, 1984.

Luther,D.S., Observations of long period waves in the tropical oceans and atmosphere, Ph.D. Thesis, Massachussetts Institute of Technology, Woods Hole Oceanographic Institution, February 1980, 210 pp.

Mangum,L.J. and S.P.Hayes, The vertical structure of the zonal pressure gradient in the eastern equatorial Pacific, J.Geophys.Res., 89, 10,441-10,449, 1984.

McCreary,J.P., Equatorial beams, J.Mar.Res., 42, 395-430, 1984.

Moore,D.W. and S.G.H.Philander, Modelling of the tropical ocean circulation, in The Sea, Ch. 8, Vol. 6, Goldberg et al. eds., Interscience, New York, 1977.

-------, D.W., Planetary-gravity waves in an equatorial ocean, Ph.D. thesis, Harvard University, 1968, 207 pp.

Overland,J.E. and R.W.Preisendorfer, A significance test for principal components applied to a cyclone climatology, Mon.Wea.Rev., 110, 1-4, 1982.

Philander, S.G.H., Instabilities of zonal equatorial currents, J.Geophys.Res., 81, 3725-3735, 1976.

-------, Instabilities of zonal equatorial currents, 2, J.Geophys.Res., 83, 3679-3682, 1978.

Romea,R.D. and R.L.Smith, Further evidence for coastal trapped waves along the Peru coast. J.Phys.Oceanogr., 13, 1341-1356, 1983.

Ripa,P.and S.P.Hayes, Evidence for equatorial trapped waves at the Galapagos Islands, J.Geophys.Res., 86, 6509-6516, 1981.

Schott,F. and W.Duing, Continental shelf waves in the Florida straits, J.Phys.Oceanogr., 6, 451-460, 1976.

Smith,R.L., Poleward propagating perturbations in currents and sea levels along the Peru coast. J. Geophys. Res., 83, 379-391, 1978.

White,W.B., G.A.Meyers, J.R.Donguy and S.E.Pazan, Short-term climatic variability in the thermal structure of the Pacific Ocean during 1979-82, J.Phys.Oceanogr., 15, 917-935, 1985.

Wang,D.P. and C.N.K.Mooers, Long coastal trapped waves off the west coast of the United States, summer 1973, J.Phys.Oceanogr., 6, 856-864, 1976.

Wunsch,C. and A.E.Gill, Observations of equatorially trapped waves in Pacific sea level variations, Deep-Sea Res., 23, 371-390, 1976.

Wyrtki,K., El Niño -- The dynamic response of the equatorial Pacific Ocean to atmospheric forcing. J.Phys.Oceanogr., 5, 572-584, 1985.

-------, The slope of sea level along the equator during the 1982/1983 El Niño, J.Geophys.Res., 89, 10419-10424, 1984.